Best
Available
Copy

AD-779 261

ARPA-NRL-LASER PROGRAM

Naval Research Laboratory

AD-779261

REPORT DOCUMENTATION PAGE		READ INSTRUCTIONS BEFORE COMPLETING FORM
1. REPORT NUMBER NRL Memorandum Report 2767	2. GOVT ACCESSION NO.	3. RECIPIENT'S CATALOG NUMBER
4. TITLE (and Subtitle) ARPA-NRL LASER PROGRAM - Semiannual Technical Report to Defense Research Projects Agency 1 January 1973 - 30 June 1973		5. TYPE OF REPORT & PERIOD COVERED A semi-annual technical Report; work continuing.
		6. PERFORMING ORG. REPORT NUMBER
7. AUTHOR(s) Laser Physics Branch		8. CONTRACT OR GRANT NUMBER(s)
9. PERFORMING ORGANIZATION NAME AND ADDRESS Naval Research Laboratory Washington, D.C. 20375		10. PROGRAM ELEMENT, PROJECT, TASK AREA & WORK UNIT NUMBERS NRL Prob. K03-08A N01-21, R08-45, K03-53 ARPA Order 2E20 (Cont'd ii)
11. CONTROLLING OFFICE NAME AND ADDRESS Defense Advanced Research Projects Agency Washington, D.C. 20350		12. REPORT DATE April 1974
		13. NUMBER OF PAGES 62
14. MONITORING AGENCY NAME & ADDRESS(if different from Controlling Office)		15. SECURITY CLASS. (of this report) UNCLASSIFIED
		15a. DECLASSIFICATION/DOWNGRADING SCHEDULE

16. DISTRIBUTION STATEMENT (of this Report)

Approved for public release; distribution unlimited.

17. DISTRIBUTION STATEMENT (of the abstract entered in Block 20, if different from Report)

18. SUPPLEMENTARY NOTES

D D C
MAY 29 1974
D

19. KEY WORDS (Continue on reverse side if necessary and identify by block number)

Lasers
Glass Lasers
Chemical Lasers
Electrical Lasers

20. ABSTRACT (Continue on reverse side if necessary and identify by block number)

The ARPA-NRL high energy laser program is concerned with the development of laser technology in four program areas; Chemical Lasers, Electric Discharge Lasers; High Power Glass Lasers and New Laser Techniques. The Chemical Laser Program has consisted of primarily two experiments; the development of $DF-CO_2$ supersonic transfer lasers, and the study of the CO vibrational distribution from exothermic reactions which produce CO. (Abstract continues)

DD FORM 1473 1 JAN 73 EDITION OF 1 NOV 65 IS OBSOLETE
S/N 0102-014-6601

i

UNCLASSIFIED

10.
Program Code 2E20
Program Element Code 62301D

20.   (Continued abstract)

The DF-CO_2 program has demonstrated chemical augmentation of a gasdynamic laser but this effect has been limited by deactivation from combustor byproducts. The initial vibrational distribution from O + CS reaction has been measured and a $V = 1 \rightarrow V = 0$ CO laser has been developed.

Assembly of the amplifier chain of the short-pulse CO_2 laser system has been completed and nominally 1 μsec pulses have been amplified to the 30 J level. Gain measurements, spatial intensity and self-oscillation problems are being addressed.

Under the New Laser Techniques Program, a fast-rising source of high energy electrons is being developed as a means for pumping visible transition laser systems.

A final report on the High Power Glass Laser Program, which summarizes the technology advances since its inception in FY-68 is given. The current status of the device for laser target irradiation up to 100 J is described.

This report covers the progress made during the second half of FY-73.

ii   UNCLASSIFIED
SECURITY CLASSIFICATION OF THIS PAGE(When Data Entered)

TABLE OF CONTENTS

FOREWORD

SEMI-ANNUAL TECHNICAL REPORT

Reporting Period

1 January 1973 - 30 June 1973

1.	DARPA Order	2062
2.	Program Code Number	2E20
3.	Name of Contractor	Naval Research Laboratory
4.	Effective Date of Contract	1 July 1972
5.	Contract Expiration Date	30 June 1973
6.	Amount of Contract	$810,000
7.	Contract Number	63201D
8.	Principal Investigator	J.R. Airey
9.	Telephone Number	(202) 767-3217
10.	Project Scientist	W. S. Watt
11.	Telephone Number	(202) 767-2028
12.	Title of Work	High Power Lasers

Sponsored by

DEFENSE ADVANCED RESEARCH PROJECTS AGENCY

DARPA Order No. 2062

CHEMICAL LASER PROGRAM

1. DF-CO_2 SUPERSONIC TRANSFER CHEMICAL LASER (TCL)

The DF-CO_2 laser operates in the 10 μ CO_2 band as a result of the
highly efficient transfer of energy from vibrationally excited DF to
the asymmetric stretching mode of CO_2. The vibrational states of
DF are preferentially excited during its chemical formation. Although
hydrogen halide chemical lasers typically operate at low pressure, the
introduction of the vibrational energy transfer process to CO_2 allows
operation at much higher pressure. This feature coupled with a super-
sonic flow offers the possibility of atmospheric pressure recovery.
Thus the DF-CO_2 TCL is of interest both as a chemical laser operating
without pumps and as a means of upgrading gasdynamic CO_2 lasers by
the addition of chemical energy to the flow.

The principle of the NRL DF-CO_2 supersonic TCL and the apparatus
acquisition and preparation have been described in previous reports
under the ARPA-NRL laser program[1,2,3]. At the beginning of the
present reporting period the apparatus had been assembled and checked
out through the initial passivation procedures. Test firings also had
been completed to ensure that complete combustion and adequate pressure
recovery were attained. These tests indicated satisfactory performance
but did not include the introduction of fluorine or deuterium into the
apparatus.

During the period covered by this report, the effort was
concentrated initially on the effect of the D_2/F_2 chemical energy
addition on the pressure recovery potential of the gas flow. The
addition of F_2 and its subsequent dissociation causes a reduction of
the temperature of the combustor gas with a corresponding increase in
the pressure. The net result was always to improve the pressure
recovery potential of the gas flow.

The addition of deuterium at the nozzle allows for the D_2-F_2
chemistry to occur in the cavity. The exoergicity of the reaction
raises the temperature and pressure of the gas in the cavity and
reduces the flow mach number. This combination of changes in the
flow properties reduces the pressure recovery potential of the flow.
To the present we have tested the addition of 1 mole sec^{-1} of D_2 and
F_2 to the flow without any measurable effect on the pressure recovery.

Following the latter experiments cavity optics were inserted for power extraction measurements. Before discussing these results, the operating sequence of the system will be described.

The device starts as an N_2-CO gasdynamic laser (GDL) with a programmed flow duration of approximately 4.3 seconds. After 1.5-seconds, if there is satisfactory achievement of preset experimental parameters, F_2 and D_2 are injected into the flow for approximately 2 seconds. The N_2 can be removed during the F_2, D_2 flow duration and replaced by a CO_2-He mixture of similar heat content. While this does not change the temperature of the gas it prevents energy transfer from N_2 to CO_2, a crucial element in the CO_2 gasdynamic laser.

Thus the output during the F_2, D_2 flow period reflects the chemical augmentation of a GDL when the nitrogen remains in the flow. When the nitrogen is removed the power corresponds to the performance of a pure DF-CO_2 supersonic laser. In either event, the output during the initial and final portions of the flow should be that of normal GDL performance of the device. This has been shown both here and elsewhere to be approximately 1.7 kW for this device

Initial experiments were conducted with an integrating calorimeter system. For true GDL operation throughout the 4.3 second test-time, the measured total output was $\sim$ 7 kJ which corresponds to 1.7 kW average power. Addition of F_2 and D_2 for 2 seconds with concurrent removal of the nitrogen lead to measured total energies in the range 9 - 10 kJ. These data were interpreted as corresponding to improved performance during the DF-CO_2 portion of the flow cycle.

Immediately following these initial tests and before time-resolved calorimetric measurements could confirm the interpretation, a series of failures in the water-cooling system led to water leakage into the laser. This problem eventually required a considerable number of parts of the apparatus to be replaced, since at various times it appeared that the problem had been overcome only to reappear elsewhere in the device. While cold-flow testing usually was sufficient to checkout the apparatus it became clear that some of the leakage problems occurred only during the high-stress period resulting during combustor operation.

The importance of keeping the combustor from leaking internally is twofold. First, water vapor in that region will react rapidly with the fluorine to produce HF. Secondly, H_2O is a very efficient deactivator of HF* and DF* and in large quantities would destroy the vibrational excitation of these molecules before it could be transferred to CO_2.

The former of these is believed to have caused us most problems. This was identified by a lack of DF in gas samples taken during the flow and the lack of any measurable effect of D_2 and F_2 addition to the gas flow properties and laser output.

It is noted here, that there is always some water vapor in the gas flow since this species catalyses the oxidation of CO to CO_2. The required H_2O is provided by the CH_4/O_2 pilot flame which is used to ignite the main combustor. This quantity of H_2O is insignificant for deactivation effects and will at most react with a part of the added fluorine.

The lack of detectable DF could possibly be explained by the difficulty one encounters in analyzing for reactive fluorine containing compounds. However, its presence in a pure GDL gas-flow, i.e. N_2 present throughout, should be apparent in the time-resolved power output. In the event that the DF is vibrationally excited it should transfer energy to the CO_2 and be observed by an increase in the power. On the other hand if it is unexcited as a result of formation within the nozzle array it should show up by a reduction in the laser power since ground state DF is known to strongly deactivate the CO_2 upper laser level[4]. Furthermore, the effect of chemistry in the supersonic flow should be seen as a rise in the pressure in the cavity and diffuser regions.

None of these effects was observed, in a number of tests, for a considerable variety of gas-flow compositions. In all cases there was no observable effect of the chemistry on the cavity pressure.

We were thus convinced of the continued presence of water leakage under the high-pressure high-temperature combustor operating conditions. As a result, further detailed examination of the apparatus revealed several suspect areas which have been modified or replaced as was appropriate.

In addition to these structural changes, the optical cavity is being redesigned to allow the incorporation of a variety of mirror sizes and locations, as well as the fixed location 8" mirror previously used. The purpose of these cavity changes is as follows. If the D_2-F_2 reaction takes place only near the nozzles then a high gain region will result in that location with low gain or loss regions further downstream in the cavity. The result of the chemistry would then have only a small effect on the output of the 8" long cavity. The use of smaller optics nearer the nozzle array would clearly take more advantage of the high gain region produced by the chemical reactions.

3

Further experiments will be conducted with the modified apparatus and cavity as described above.

NOTE: In recent tests with 1" optics located just downstream of the nozzle array, increased power and increased cavity pressure have been detected when D_2 and F_2 were injected into the gas flow.

2.   CO POPULATION DISTRIBUTIONS

The direct measurement of the initial vibrational distribution of CO produced from O + CS by the intracavity laser probing method has been successfully completed.   In addition we have discovered the means to achieve cw CO laser oscillation on the lowest vibrational bands down to $V = 1 \rightarrow V = 0$.

During the second half of FY-73, a completely new CO probing system was constructed.   This required the design and fabrication of a probing CO laser which could be operated in the lowest vibrational transitions and the construction of a transverse-flow reactor which would provide a minimum residence time for the CO product molecules. After some experimentation, it was found that the low-lying CO vibrational bands could be made to oscillate when one used for the active medium a He-N_2-CO-Xe mixture with a large N_2 to CO ratio ($\geqslant 100$).   It appears that the Xe produces a more favorable electron distribution for vibrational excitation and the high N_2 to CO ratio insures a low net rate of loss of vibrational energy.   Single line TEM$_{oo}$ output of a few milliwatts can be obtained on about half a dozen P-branch transitions in each band down to $V = 1 \rightarrow V = 0$. Further details on this laser can be found in the Applied Physics Letters reprint included in Appendix A.

Since the feasibility of the experiment depended largely on the sensitivity of the intracavity method, it was decided to calibrate the detectivity of the system first.   This was done by filling the reactor with known concentrations of CO and monitoring the loss due to the very small fraction of CO in the $V = 1$ level.   The results indicated that the system was capable of measuring gain or loss as small as three hundredths of one percent.   This figure corresponds to a detectivity of about 10^9 cm^{-3} (over a 10 cm path) for the population difference between a pair of vibration-rotation levels at $V \simeq 10$.

The transverse flow reactor had four parallel 6 mm x 10 cm channels which fed into the reaction plenum in a plane 19 mm upstream from the optical axis.   The two middle channels were used for the injection of O and CS which were produced further upstream in separate electric discharges.   Nitrogen flowed through the outer channels

4

to create a diffusion barrier between the reaction zone and the vessel walls. The average residence time of a CO molecule before crossing the optical axis was estimated to be 0.3 msec. For a total pressure of slightly over 1 torr, the effect of wall deactivation was insignificant. For CO partial pressures of under 10^{-3} torr, V-V relaxation was also found to be negligible. The measured CO initial vibrational distribution is a skewed bell-shaped curve with its peak at V=12 and falling off to nearly zero at V = 0 and V = 16. These results are in almost complete agreement with some earlier ones obtained through extrapolation by Hancock et al[5]. The data acquired in these experiments provide the starting point for any modelling calculation on the O_2-CS_2 chemical laser system.

The details of this experiment are being written up presently for publication.

3. CO VIBRATIONAL ENERGY TRANSFER MEASUREMENTS

It was discovered that there was a chance coincidence between frequency doubled CO_2 laser lines and certain fundamental lines in the CO spectrum. Consequently, for the first time, laser induced fluorescence studies of CO collisional relaxation have been carried out using the output of a frequency-doubled, pulsed CO_2 laser as a direct source of CO(v=1) excitation. Energy transfer cross sections at 298°K are reported for CO in collisions with He, Ar, H_2, D_2, N_2, O_2, Cl_2, NO, CH_4, CF_4 and SF_6. The D_2-D_2 self-relaxation rate was also obtained from the analysis of CO-D_2 mixtures.

REFERENCES

1. NRL-ARPA Laser Program Semi-Annual Technical Report, 1 January 1972 - 30 June 1972, NRL Memo Report No. 2483.

2. NRL-ARPA Laser Program Semi-Annual Technical Report, 1 July 1972 - 31 December 1972, NRL Memo Report No. 2529.

3. NRL-ARPA Laser Program Semi-Annual Technical Report, 1 January 1973 - 30 June 1973, NRL Memo Report No. 2654.

4. R.R. Stephens and T.A. Cool, J. Chem. Phys. 56, 5863 (1972).

5. G. Hancock, C. Morley and I.W.M. Smith, Chem. Phys. Letters 12, 193 (1971).

SHORT-PULSE CO$_2$ MOLECULAR LASER

The goal of this program is to build a 30 joule, 1 nanosecond pulse laser system at 10 μm. A train of nanosecond pulses is produced in a helical pin TEA laser, which is actively mode-locked using a Brewster-Bragg Ge modulator driven by a LiNbO$_3$ transducer. Careful control of the drive frequency and power, and the laser discharge parameters, results in stable production of trains of pulses with widths $\sim$ 1 nsec. Pulse widths are measured using a high speed photon-drag detector and a Tektronix 7904 oscilloscope with combined risetime $\leq$ 1.2 nsec. Single pulse selection is achieved using a GaAs Pockels cell placed between crossed stacked-plate Ge polarizers. The extinction ratio of unwanted polarization with this arrangement is better than 32 db. The Pockels cell is activated by a high voltage pulse from a laser triggered spark gap. The selected pulse energy is typically $\sim$ 2 mJ.

This pulse is first amplified to an energy $\sim$ 2 J in a series of five Pearson-Lamberton type distributed discharge TEA amplifiers. The total small signal gain of these amplifiers has been measured to be $\sim$ 41 db. Gain measurements were carried out on individual stages using a stable cw laser operating on the P(20) transition of the 10.6 μm band of CO$_2$. After beam expansion the pulse is further amplified in two Lumonics Series 600 amplifiers (total small signal gain $\sim$ 15 db) to an energy $\sim$ 10 J with a beam area $\sim$ 33 cm^2. Problems associated with self oscillation of the amplifier-chain were avoided by careful alignment of the amplifier stages to avoid reflections from the lucite walls of the amplifier boxes and from the edges of the profiled electrodes. The output beam contains some spatial intensity modulation due to diffraction at the amplifier electrodes.

Work is at present under way to characterize the spectral and temporal properties of the pulse at various stages of amplification and to improve the spatial profile of the output beam.

The final amplifier will be a 10-liter discharge controlled by a cold-cathode electron beam. Delivery of this amplifier has been delayed twice, with delivery now scheduled for August 1973.

Note: The final amplifier was installed in the system in August. Preliminary measurements indicate that the pulse energy after final stage amplification is $\sim$ 33 J.

NEW LASER TECHNIQUES

E-BEAM INITIATED VISIBLE TRANSITION LASERS

Visible transition lasers can be pumped effectively by fast-rising powerful pulses of high energy electrons. The fast risetime is required to overcome the high relaxation rates and short lifetimes associated with electronic states. The high power is required to create a sufficient density of electronically excited species. During this reporting period, an e-beam device for laser pumping was constructed and tested. Typically, the e-beam gave pulses with a risetime of 8 ns, a pulse length of 50 ns, a peak voltage of 500 kV, and a peak current of 40 kA. These numbers correspond to an energy of 1 kJ per pulse. Approximately 10% of the electrons reach the laser cell after passing through the screen anode, foil support plate, and one mil thick titanium foil window. In the laser cell the electrons are stopped with an energy loss rate of $\sim 0.5\%$/cm-atm for 500 kV electrons. Complete absorption of the beam by the gas in the cell would result in the production of 10^{20} ion pairs and about 10^{20} excited neutral species, formed in a volume 15 cm long (the width of the e-beam) by 1 cm thick (determined by the diameter of the holes in the foil support plate) by a depth determined by the gas pressure.

The high voltage engineering work began with the problem of characterizing the performance of an LC generator coupled to an 8 ohm water-filled folded-Blumlein transmission line terminated in a vacuum diode. This system was constructed in the first half of FY-73, but its characterization was delayed due to the failure of a number of components. These components included a capacitor in the energy storage bank which fired on a random basis, the elkonite tip of the water gap switch which loosened from the main body of the switch, and prepulse hold-off plates which broke down internally. After component reliability was established, the proper settings for the switches were determined as a function of the charging voltage. Finally the anode-cathode spacing was varied to determine impedance of the diode and to optimize the electron emission. The problem is complex because the charging voltage will double by reflection from a high impedance load, the diode. Thus achievement of the necessary 400 kV/cm electric field gradient must be ascertained experimentally.

A number of different anodes, foil holders, and foils have been evaluated. The present arrangement has a high transmission screen anode and a foil holder 3/8" thick with one centimeter diameter holes closely spaced along a line 15 cm long. The electrons which pass

7

through the foil enter a cell fitted with Brewster angle windows which
form an optical axis transverse to the electron beam. Photodiode
detectors are used to monitor the electron beam induced emission.

In conclusion the overall performance of the e-beam device is
very good compared to any other similar device.   Component failures
are expected to be only a minor problem in the future.   Thus a major
portion of the time during the next six months can be spent on e-beam
initiated laser experiments.

HIGH POWER GLASS LASER PROGRAM

This is the final report on the glass laser program, since ARPA support of this project was terminated at the end of this reporting period. This program was initiated in FY-68 and has paced the development of high power glass laser technology since that time. Initially, amplification processes in rod amplifiers, development of a bandwidth limited Nd:YALG oscillator and the formulation of a Monte Carlo optical-power flow code were addressed. Subsequently, a disc amplifier, designed with the aid of this code, was built and tested. This led to an intensive effort to understand the self-focusing damage problem in high power glass systems and the limitations on energy storage in glass discs due to parasitic oscillation.

LASER OPERATION AND DEVELOPMENT

At the onset of the year it was obvious that the NRL glass laser system would have to be capable of sustained performance over a wide range of parameters. Program analysis revealed that there were several subsidiary goals necessary to achieve the desired laser performance for the DNA photon sources program and the AEC laser induced fusion program:

- isolation of the system from back reflections from the target

- prepulse generation for the system and a study of the relative merits of more complicated pulse shaping schemes

- improved beam control to minimize self-focusing damage

- component re-engineering to reduce routine maintenance costs

- complete disc amplifier characterization to determine the scalability of this approach.

Not all of these goals were pursued on ARPA funding. The isolation system was initiated on AEC funding while ARPA funded the disc amplifier work and some of the beam control work. Since all of these goals had to be met to have a reliable working laser system we will also summarize relevant work performed for other sponsors in this report.

The schedule we have attempted to follow this year has been 2/3 time for target experiments and 1/3 time for routine laser maintenance and testing improvements to the system. There have been in excess of

9

3000 shots on the system with over 2000 shots on target. Approximately 70% of these shots were at energies below 20 J on target before the isolation system was installed with 30% of the shots at 20 - 100 J on target since the system isolation was installed.

In October target runs will commence at 100 - 200 J on target. Also, the first redesigned disc module will be delivered and operation will commence at the 200 - 300 J level on target with routine operation at this level scheduled by mid-year.

The isolation system uses an optimized mix of Pockel's cells and Faraday rotator isolators. Two Pockel's cells are used to extract a pulse from the modelocked pulse train generated by the oscillator and to suppress any prelase or unintentional preirradiation of the target. Commercially available Faraday rotators suffered from two serious flaws; they were very expensive and the extinction ratio was very low (e.g. 17 db for the CGE FR-70). We therefore designed and built standardized 8 cm aperture Faraday rotators for our system. An extinction ratio of 35 ± 1 db was achieved in a straight forward fashion in a rotator design which should be sensibly immune to self-focusing damage. Appendix C summarizes the Faraday rotator design and performance in more detail. The system is currently running with two of these rotators installed. The third rotator (built with AEC and DNA funding) will be installed for operation at levels in excess of 200 J on target.

A simple optical-delay-line prepulse generator is in use on the system and experiments are underway to determine optimum values for delay and relative energy. A comprehensive review of applicable techniques for shaping of laser pulses has been performed and two techniques identified which offer sufficient control to achieve any desired shape. Such techniques also appear to offer the possibility of easing the restriction on laser power density caused by self-focusing. We are pursuing a feasibility demonstration in this area as it appears that it could favorably impact the efficiency of high energy short pulse lasers by a factor of three to five.

The self focusing problem has been investigated further and suppressed to the point where no single-shot damage is apparent in the system. After 400 - 500 shots sufficient damage accumulates in the 45 mm amplifier that it must be replaced. This represents a cost of $12-15/shot for laser glass which is quite acceptable. The cause of this problem is self-focusing of spatial structure on the beam due to diffraction, misalignment, and materials imperfections. Appendix D summarizes our approach to minimizing this problem which has been relatively successful (AEC, ARPA, DNA funding).

10

Disc amplifiers and similar geometries (e.g. stacked plate polarizers) have a serious failing from a routine maintenance standpoint; they have a large number of optical surfaces which must be kept scrupulously clean. Even with electrostatic precipitators in the laboratory all surfaces must be cleaned at least once a week. Reduction of the amount of cleaning required is mandatory for a viable laser.

The first step towards this goal was a sealed stacked plate polarizer. The plates were cleaned and assembled in a dust free room. This assembly has been in the system for four months (~ 1000 shots) and there has been no damage or degradation of the passive transmission of the device.

The second data point was a sealed helically-pumped 44 mm aperture disc amplifier (which will replace the 64 mm rod amplifier). Initial operation of this amplifier was nominally successful, but it was found that over a number of shots the inner wall of the Pyrex cladding-jacket ablated material onto the discs. It was also found that O-ring seals had to be carefully assembled to avoid ablation of O-ring material on to the discs.

The redesigned 66 mm disc-amplifier modules incorporate what has been learned from these experiments. It is a sealed geometry with a filtered dry-nitrogen purge and with a fused-silica cladding-jacket. The first module will be delivered for testing in October (ARPA funding).

Over the past year a number of experiments have been run to characterize the performance of the present 66 mm disc amplifier. It has additionally been used for all the routine target operation at energies above 20 J. Several questions have been addressed which are of some importance for high energy short pulse lasers:

- is the performance understood?

- how much degradation is there in routine operation?

It was found that the energy storage could be parametrized by the ZAP optical-pumping code and the energy extraction could be predicted using a rate equation approach. The agreement with theory and the generability of the techniques used were such that it appears that disc laser technology can in fact be scaled to the multikilojoule level with a high confidence factor.

All the degradation found in routine operation was tracible to the condition of the disc surfaces. Performance returned to initial levels when the discs were cleaned or repolished. Careful investiga-

tion did not reveal the presence of any systematic degradation mechanisms. The techniques used were sensitive enough that a change in transmission of 0.5%/cm would have been observable. This research is summarized in Appendix E. The degradation we have encountered can be eliminated by careful mechanical design such that the discs are in a clean, sealed environment. This feature is incorporated in our new design (ARPA funding).

The NRL short pulse laser has been used and improved to the point where several thousand shots/year at energies up to 300 joules on target will be available with a minimum of maintenance and low operating costs. The technology which has been developed to enable this performance is directly scalable to higher output levels.

In summary, the ARPA-NRL glass laser program has helped pace the technology in reliable high peak power short pulse lasers from 2 GW in 1968 to 1 - 2 TW in 1973. The technology has matured to a point where the laser is now a tool for experiments and not the experiment. Specific areas of impact of the ARPA-NRL program have been in systems modelling and numerical simulation of lasers, reliable short pulse oscillators, self-focusing studies, and high efficiency large aperture disc amplifiers. Most of the laser technology base for the AEC laser pellet fusion program at Livermore has been generated on this program.

APPENDIX A

CW SINGLE LINE CO LASER ON THE V = 1 → V = 0 BAND*

N. Djeu

Laser Physics Branch
Optical Sciences Division

Naval Research Laboratory
Washington, D.C. 20375

ABSTRACT

CW single line laser oscillation has been achieved on the P(9), P(10) and P(11) transitions in the V = 1 → V = 0 band of CO. The observations were made on a conventional electrical discharge, slow-flow device filled with a mixture of He, N_2, Xe, and CO.

This paper describes the first successful operation of a cw single line CO laser on the V = 1 → V = 0 band in the ground electronic state. Such a laser makes it possible to further test a number of theories on the interaction of highly coherent radiation with molecules by allowing the use of ground state CO as an example. The 1 → 0 laser will also be a useful tool for monitoring ground state CO concentrations. Furthermore, the tunability of the present laser over the other low lying bands of CO renders it an ideal source for atmospheric transmission experiments in the 5 μ region.

It is known that in a mixture of vibrationally excited N_2 and CO, the latter can have an appreciably higher 1 → 0 vibrational temperature by virtue of its smaller vibrational quantum[1,2]. This effect is readily visualized in terms of the quasi-steady vibrational distribution for a pure anharmonic gas. Such a distribution is characterized by the vibrational temperature between adjacent levels becoming progressively greater with V (up to the point where the inversion ratio is just under unity). When a second anharmonic gas with somewhat lower frequency is added to the first, one can imagine that all the vibrational levels above a certain V in the original gas have now in effect become "degenerate". The energy of the V = 1 → V = 0

transition in CO is resonant with that of $V = 7 \rightarrow V = 6$ in N_2. Therefore, as far as V-V energy exchange is considered, a CO molecule in the ground state is equivalent to a N_2 molecule in the $V = 6$ level. Hence the inversion ratio between $V = 1$ and $V = 0$ can be expected to be much higher for CO than for N_2 in a vibrationally excited mixture of the two gases.

That very high inversion ratios for the low-lying bands in CO can indeed be achieved has been demonstrated in a fast-flow N_2-CO mixing apparatus[3]. The present experiment shows that the same effect is obtained in a premixed, essentially non-flowing system. Moreover, it is found that the inversion ratios can be increased further by the use of Xe in the discharge. This supports the conclusion by Bhaumik et al that Xe alters the electron energy distribution in such a way as to promote the vibrational excitation of N_2[4].

Some construction features of the present laser are shown in Fig. 1. Two main conditions desired are the liquid nitrogen cooling of the entire laser active length and the avoidance of ground state CO beyond the discharge region. Both are essential for the operation of the CO $1 \rightarrow 0$ laser. The CO self-absorption problem was solved by flowing He in through sidearm B and the rest of the gases in through sidearm A. In addition, a piece of 10 mm i.d. Teflon was inserted into the 20 mm i.d. Pyrex laser tube just outside of the discharge. This last step aided in the prevention of back diffusion of CO into the unexcited region. The laser tube had two anodes near the ends and a cathode in the middle. Gases were removed from the tube through a port near the cathode by means of a 13 c.f.m. pump. The entire active region was 1.5 m in length. The laser cavity consisted of a 300 lines/mm grating blaced for 4 μ and a nominally 2% transmitting curved mirror.

Laser oscillation on three lines in the $V = 1 \rightarrow V = 0$ band was obtained with 5 torr He, 1.5 torr N_2, 0.1 torr Xe, and 0.01 torr CO with a total current of 15 mA. The measured wavelengths in air of 4.744 μ, 4.753 μ and 4.763 μ identified these lines as the P(9), P(10), and P(11) transitions in the $V = 1 \rightarrow V = 0$ band. To verify that the laser transitions indeed terminated on the ground vibrational level of CO, a resonance absorption test was made on the three lines. A 20 cm long cell was placed between the output mirror and the detector. The filling of the cell to a few tens of mtorr with CO absorbed the output almost entirely, proving conclusively the nature of those laser transitions. The TEM_{oo} mode output at line center for each of the $1 \rightarrow 0$ lines was measured to be about 5 mW. Oscillation was also observed on at least six lines, centered around P(9), for each of the higher bands. The output power from the latter were generally greater than those from the $1 \rightarrow 0$ transitions.

When the CO partial pressure was increased from 0.01 torr, with the current kept at 15 mA, laser output on the $1 \rightarrow 0$ transitions became weaker. At a CO pressure of about 0.02 torr, no laser action was possible on any of the $1 \rightarrow 0$ lines. These observations can be explained by the following arguments. The steady state N_2 and CO vibrational distributions are determined by the rates of vibrational excitation by electron impact, etc., on the other hand and vibrational deactivation via V-T exchange and radiative decay on the other hand. It is reasonable to assume that an addition of 0.01 torr of CO to 1.5 torr of N_2 brings about a negligible change in the excitation rate of the latter. However, the probability of vibrational deactivation for CO is much greater than that for N_2. Hence, even a small amount of CO in an N_2-CO mixture would contribute heavily towards the relaxation of the whole. A large fractional increment in the CO pressure could therefore result in significantly lower inversion ratios in the mixture.

In conclusion, then, it has been demonstrated that a CO laser operating on the $V = 1 \rightarrow V = 0$ band can be easily built. Such a laser should find numerous applications in quantum optics and related fields.

REFERENCES

1. C.E. Treanor, J.W. Rich, and R.G. Rehm, J. Chem. Phys. 48, 1798 (1968).

2. G.E. Caledonia and R.E. Center, J. Chem. Phys. 55, 552 (1971).

3. N. Djeu, Chem. Phys. Lett. 15, 392 (1972).

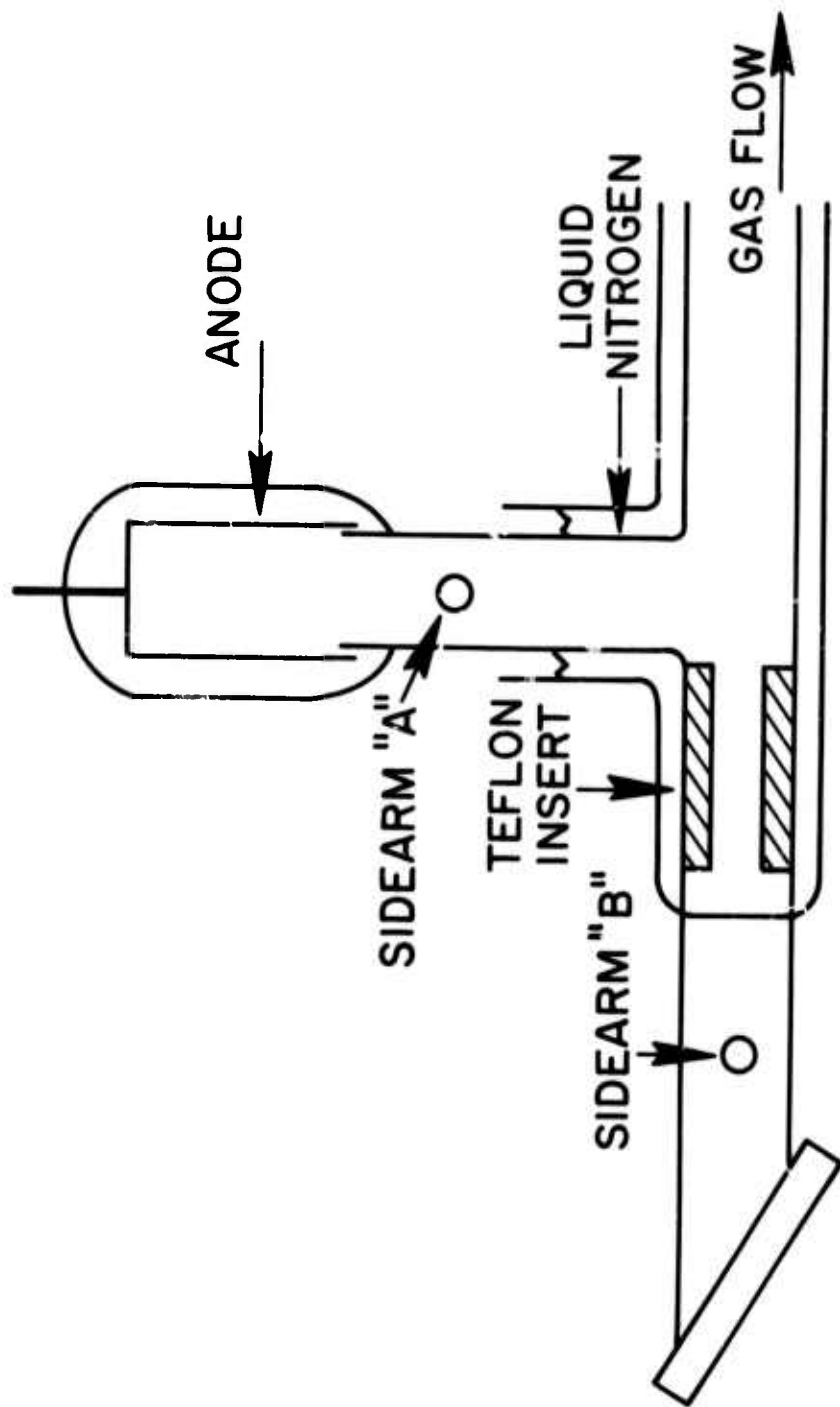4. M.L. Bhaumik, W.B. Lacina and M.M. Mann, IEEE J. Quantum Electronics QE-6, 575 (1970).

Fig. 1 - Details of laser construction near one anode.

ANODE

LIQUID
NITROGEN

GAS FLOW

SIDEARM "A"

TEFLON
INSERT

SIDEARM "B"

THE JOURNAL

OF

CHEMICAL PHYSICS

Measurement of CO(v = 1) vibrational energy transfer rates using a frequency-doubled CO₂ laser

W. H. Green and J. K. Hancock

Chemistry Division U. S. Naval Research Laboratory, Washington, D.C. 20375

Published by the

AMERICAN INSTITUTE OF PHYSICS

Measurement of CO(v = 1) vibrational energy transfer rates using a frequency-doubled CO₂ laser

W. H. Green and J. K. Hancock

Chemistry Division U. S. Naval Research Laboratory, Washington, D.C. 20375

(Received 6 July 1973)

Laser-induced fluorescence studies of CO collisional relaxation have been carried out using the output of a frequency-doubled, pulsed CO₂ laser as a direct source of CO(v = 1) excitation. Energy transfer cross sections at 298 °K are reported for CO in collisions with He, Ar, H₂, D₂, N₂, O₂, Cl₂, NO, CH₄, CF₄, and SF₆. The D₂–D₂ self-relaxation rate was also obtained from the analysis of CO–D₂ mixtures.

INTRODUCTION

Studies of collisional processes in gases have expanded remarkably in the past decade as a result of the introduction of gas lasers and the accompanying impetus toward their further development. A primary requisite for the understanding and improvement of lasers in a comprehensive knowledge of how rapidly or effeciently the excited lasing species exchanges energy in collisions with itself and with other species present in the laser medium. Recent advances in CO laser technology have enhanced interest in acquiring such a detailed picture with respect to CO energy transfer. We report here a new technique which allows CO(v = 1) relaxation rates to be obtained via the laser-induced vibrational fluorescence method along with some of the initial rate data thus extracted.

The landmark experiments of Millikan initially established that measurements of the quenching of vibrational fluorescence can provide vibrational energy transfer cross sections.[1] Millikan utilized a continuous blackbody or CH₄/O₂ flame source to excite a flowing sample of CO to a vibrational temperature near 1000 °K, while retaining an ambient translational, rotational temperature. The ensuing steady-state fluorescence intensity was determined and then monitored as a function of pressure of added quenching species. From a knowledge of the spontaneous emission lifetime of CO(v = 1) and a Stern–Volmer analysis, CO vibrational energy transfer rates were derived for a number of additives.

Subsequently, Hocker, Kovacs, Rhodes, Flynn, and Javan[2] and Yardley and Moore[3] almost simultaneously expanded the concept by performing experiments in which a *pulsed* CO₂ laser was used to excite vibrational fluorescence from CO₂(001). The decay of fluorescence intensity with time permitted vibrational relaxation to be measured in "real time." The laser-fluorescence technique was extended to the investigation of other molecules as the appropriate pulsed laser sources became available. For the most part, however, the lack of continuous tunability of gas lasers has restricted study to those molecules for which lasers operating on the transition to be pumped, existed. Such was the case for the hydrogen and deuterium halides which were examined after the corresponding chemical laser sources were developed.[4]

Although CO lasers have been around for some time, they only operate on transitions originating from CO(v > 1)[5] and, because of anharmonicity, do not overlap the fundamental transition of CO (an analogous situation pertains for the NO molecule). Nevertheless, a substantial number of CO V → V rates have been successfully inferred from the data obtained for Mᵗ–CO gas mixtures excited with a "M" laser (e.g. M = CO₂, N₂O, DCl, and HBr).[6] In these cases the M → CO V → V rate was measured from the decay of M fluorescence, and the reverse CO → M V → V rate was calculated from the principle of detailed balancing. Additionally, laser excited HF[7] and DCl[8] have been used as collisional pumps of the CO(v = 1) level which in turn was quenched by a third molecule. This latter method provided the first room temperature measurements of the CO → N₂[7,8] DBr, DI, and CD₄[9] V → V rates. A major drawback of the indirect laser experiments is the limitation to those mixtures of gases which possess a pumpable species and a fortuitous interrelation of rate constants that is amenable to analysis.

In addition to the fluorescence methods discussed above, the diverse techniques of flash kinetic spectroscopy,[10] shock tube,[11] ultrasonics,[12] the spectrophone,[13] chemiluminescence,[14] pulse-gain,[15] and stimulated Raman scattering[16] have been applied to the study of CO relaxation with varying degrees of success. Although each of these techniques is uniquely indicated for certain applications, the indirectness, serious assumptions, extrapolations, or other limitations often involved detract from their utility for the study of CO(v = 1) relaxation near room temperature and below.

Dubost, Abouaf-Marguin, and Legay[17] recently showed that a frequency-doubled CO_2 laser could successfully pump and produce fluorescence from the broad fundamental transition ($\Delta\nu \sim 0.8$ cm^{-1}) of matrix-isolated CO. Subsequently, Hancock and Green[18] and Stephenson[19] independently showed that the same technique could be used to excite fluorescence from *gaseous* CO due to the fortuitous coincidences of two frequency-doubled CO_2 laser lines to within ~ 0.01 cm^{-1} of the $R(2)$ and $P(14)$ transitions of CO. Likewise, Stephenson has recently achieved direct excitation of gaseous NO.[20] Hence, direct laser-induced fluorescence experiments of CO and NO are now possible.

This paper reports energy transfer rates for CO – He, Ar, H_2, D_2, N_2, O_2, Cl_2, NO, CH_4, CF_4, and SF_6. It was also possible to use $CO(v=1)$ as a collisional pumping source to allow determination of the $D_2(v=1)$ self-relaxation rate. In general, our data show good agreement with the steady state values of Millikan, and excellent agreement with the very recent data of Stephenson.

EXPERIMENTAL

Frequency doubling or second-harmonic-generation (SHG) is a nonlinear process which can occur when a high intensity laser beam is passed through a phase-matched birefringent crystal. Phase-matching is attained when the refractive index of the crystal at the incoming fundamental and outgoing doubled frequencies is identical along the path that the photons travel through the crystal. Details of SHG may be found in the literature.[21]

In order to achieve the power densities required for SHG, a CO_2 TEA laser was selected as the pump laser source. The laser was fabricated from a 56 mm i.d., 1.3 m length Lucite tube with Brewster angle NaCl windows attached at each end. The tube was wrapped with two helices of 1000 W resistors which served as anode and cathode. Individual resistors were spaced 8 mm apart and connected in parallel at one end; the other end of each resistor extended through a drilled hole into the tube a distance of 15 mm. The configuration of the helices was such that each anode resistor "pointed" to a corresponding cathode resistor on the opposite side of the tube. The TEA laser power supply consisted of an RC discharge network (0.04 μf, 15 kv) which was fired by a hydrogen thyration at repetition rates variable from manual to ~ 50 pps.

The laser cavity was comprised of a 10.6 μ master grating and a 5 m radius germanium output coupling mirror that was dielectrically coated for 25% transmission at 9.6 μ. Irises were placed between the laser tube and the grating and mirror and adjusted to attain a uniform circular beam intensity profile from a single vibration-rotation transition of CO_2. Specifically, when the $P(24)$ and $R(18)$ lines of the $CO_2(001-020)$ transition are doubled they almost exactly coincide with the $P(14)$ and $R(2)$ transitions of CO, as shown in Table I.

A high purity, single crystal of tellurium (hexagonal profile), originally obtained from the Wacker Chemical Company of Germany as a boule, was chosen as the doubling medium. A 12 mm section of the boule was sliced with parallel surfaces cut at a $16°$ angle to the c axis for phase-matching at 9.6 μ. The crystal was hand polished, and then installed in a conventional adjustable mirror mount and aligned with the TEA laser output. It was determined that the crystal doubled $\sim 0.1\%$ of the input radiation to produce ~ 10 μJ, 300 nsec FWHM pulses at 4.8 μ.

High sample purity is mandatory in energy transfer studies, particularly in the case of CO which is known from earlier measurements to have relatively slow $V\rightarrow R$, T relaxation rates. A very small impurity which contains a vibrational degree of freedom that is nearly resonant with $CO(v=1)$ can lead to erroneously fast $V\rightarrow R$, T results. The states impurities in ppm of our Matheson gases were the following:

Research Grade CO (99.9%): <10 H_2, <20 O_2, <20 Ar, <100 N_2, <10 CO_2; <10 H_2O, <2 hydrocarbons;

Matheson Grade He (99.9999%): <5 Ne, <1 N_2, <1 O_2, <1 Ar, $<$ H_2, <0.5 CO_2, <0.6 H_2O, <0.5 hydrocarbons;

Matheson Grade Ar (99.9995%): <5 N_2, <1 O_2, <1 H_2, <0.5 CO_2, <0.6 H_2O, <0.5 hydrocarbons;

Research Grade O_2 (99.99%): <20 N_2, <20 Ar, <10 CO_2, <5 N_2O, <15 Kr, <5 Xe, <6 H_2O, <20 hydrocarbons;

Research Grade N_2 (99.9995%): <1 O_2, <1 H_2, <1 Ar, <1 Ne, <0.5 CO_2, $<$ H_2O, <0.5 hydrocarbons;

C. P. Grade D_2 (99.5%): 300 N_2, 5 O_2, 1000 HD, <1 hydrocarbons;

Research Grade Cl_2 (99.965%): <100 N_2, <50 O_2, <200 CO_2, <3 H_2O;

Research Grade CH_4 (99.99%): $< 20 \, N_2$, $< 10 \, O_2$, $< 6 \, H_2O$, $< 55 \, C_2H_6$;

Ultra High Purity H_2 (99.999%): $1 \, O_2$, $1(CO + CO_2)$, 50 He, $5 \, H_2O$, < 0.8 hydrocarbons;

C. P. Grade NO (99.2%): $2000 \, CO_2$, $5000 \, N_2$, $500 \, N_2O$, $500 \, NO_2$;

Matheson Grade CF_4 (99.7%): $< 15 \, H_2O$, $< 1.5\%$ air;

Instrument Grade SF_6 (99.99%).

In the case of bottled gases new, unused regulators were installed. For those gases expected to be very slow quenchers, high purity metal diaphragm regulators were employed.

Gas samples were prepared and mixed in a greasless, bakeable vacuum system which was constructed of Pyrex tubing and Teflon stopcocks fitted with Viton O-rings. Pressure measurements were made with a Granville-Phillips ionization gauge (10^{-3}–10^{-9} torr), a Wallace-Tiernan differential pressure gauge (0–20 torr) and a mercury manometer (0–800 torr). The condensible gases (Cl_2, NO, CF_4, and SF_6) were freeze-pumped and outgassed at 77 °K. After several freeze-thaw cycles a middle fraction of the slowly warming up vapor was withdrawn for sample use. C. P. grade NO was further purified by the procedure discussed in an earlier paper.[7] Noncondensible gases (CO, He, Ar, H_2, D_2, N_2, O_2, and CH_4) were placed in baked-out 2 liter glass bulbs with large "cold feet" that were immersed in liquid nitrogen for several hours before use.

The fluorescence cell was fabricated from oxygen-free copper stock. Ceramasil sapphire window assemblies were silver-soldered into position. Prior to sample introduction the cell was baked and pumped to $< 10^{-5}$ torr and an outgassing rate of $< 10^{-5}$ torr/h. As a system check, a comparison of data from several samples studied soon after mixing and again after standing in the cell for over 24 h showed no measurable differences in relaxation times.

Fluorescence signals, monitored with an InSb PEM detector, were passed through a Perry Model 720 preamplifier and displayed on a Tektronix 535

oscilloscope which incorporated a model 1A7A amplifier. Scope traces were recorded photographically via a Tektronix C-12 camera with a projected graticule. The doubled laser power produced ample "single-shot" fluorescence from CO such as to make signal averaging totally unnecessary (e.g., see Figs. 1 and 2). It has been shown[24] that excessive production of AB($v = 1$) molecules by a laser can be followed by rapid vibrational laddering to higher vibrational levels. Fluorescence from these higher levels can cause an anomalous shortening of the observed fluorescence lifetimes when $E_{vib} \gg E_{rot,trans}$, as is the case for room temperature laser-fluorescence experiments.[25] In order to ascertain that this complication was not present, a test was performed in which a 10-cm long gas cell was placed between the sample cell and the detector. It was found that the cell attenuated ~95% of the fluorescence intensity upon being filled with 1 atm of CO, and thus that fluorescence from $CO(v > 1)$, which should be transmitted through the cell unattenuated, did not make a significant contribution to the measured signals.

Sample pressures and associated relaxation times of CO-additive mixtures are listed in Tables II and III.

DATA ANALYSIS

Mixtures of CO with all additives except D_2 and N_2 exhibited the single exponential CO fluorescence decay indicative of "one-way" vibrational relaxation. The analysis of such decay is straightforward using the following familiar relationship:

$$\tau_{observed}^{-1} = k_{CO-CO} P_{CO} + k_{CO-X} P_X + \tau_{radiative}^{-1}, \quad (1)$$

where τ's are the experimental and spontaneous

TABLE I. Frequency match of doubled CO_2 and $CO(v = 0 \rightarrow v = 1)$.

CO_2 laser transition	Doubled (cm^{-1})[a] frequency	CO transition	Frequency[b] cm^{-1}	$\Delta\bar{\nu}$(cm^{-1})
$(001) \rightarrow (020)$ $P(24)$	2086.326	$P(14)$	2086.323	0.003
$R(18)$	2154.605	$R(2)$	2154.598	0.007
$R(30)$	2169.270[c]	$R(6)$	2169.200	0.070

[a]See Ref. 22.
[b]See Ref. 23.
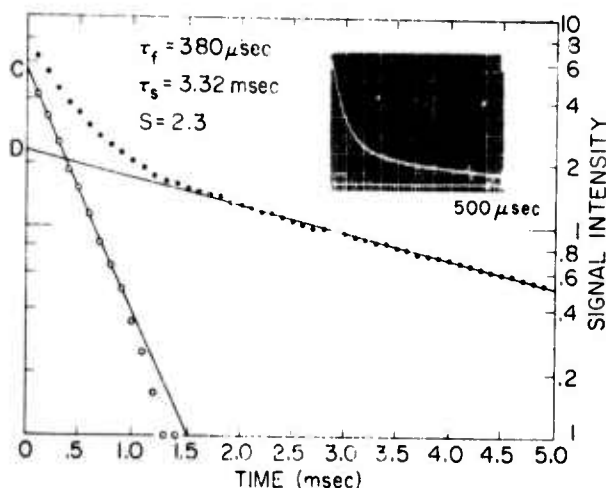[c]This line has produced fluorescence in pressure broadened CO samples.

FIG. 1. Semilog display of double exponential decay observed in a CO–D_2 mixture, (inserted is a photograph of the original oscilloscope trace on a 500 μsec/cm time scale); $S = C/D$.

emission lifetimes, P = pressure in torr, and the k's are rate constants in second$^{-1}\cdot$torr^{-1}. The CO self-relaxation rate, k_{CO-CO}, is found to be 2.3 $\times 10^{-4}$ sec$^{-10}\cdot$torr^{-1} from an extrapolation of the shock data of Hooker and Millikan,[11] and $(1.9 \pm 0.6) \times 10^{-3}$ sec$^{-1}\cdot$torr^{-1} from the stimulated Raman scattering work of Kovacs and Mack.[16] In either case k_{CO-CO} is orders of magnitude smaller than k_{CO-X} for all the mixtures studied here, so to an excellent approximation the $k_{CO-CO}P_{CO}$ term may be set equal to zero. Furthermore, collisional processes generally dominate CO relaxation so that $\tau_{obs}^{-1} \gg \tau_{rad}^{-1} = 1/30$ msec, and the last term in Eq. (1) may properly be ignored. Nevertheless, the experimental lifetimes measured for the CO–He and CO–Ar mixtures are sufficiently long that τ_{rad}^{-1} may not be neglected. Unfortunately, radiation trapping, which is expected to occur under the present experimental conditions, can lead to an uncertain lengthening of τ_{rad} beyond the 30 msec value that is valid in the zero pressure limit. As a consequence, the exact amount of the correction due to spontaneous emission is not known. Rather than make an approximate correction to the measured rate constants in Tables II and III, the error limits have been expanded to cover the maximum uncertainty that $\tau_{rad} \geq 30$ msec could create.

In effect Eq. (1) is then reduced to

$$\tau_{obs}^{-1} = k_{CO-X}P_X. \tag{2}$$

The constant k_{CO-X} is the sum of the specific rates of each available quenching channel: for monatomic additives k_{CO-X} is simply a $V \to T$ rate; for diatomic additives, $k_{CO-AB} = k_e^{V \to V} + k_{CO-AB}^{V \to R,T}$; and for polyatomic collision partners,

$$k_{CO-poly} = \sum_{v=1}^{3N-5,6} k_{e_i}^{V \to V}i + k_{CO-poly}^{V \to R,T}.$$

The vibrational and rotational–translational channels are not separable by the analysis above since each specific rate is linearly dependent upon additive pressure P_X; however, with the exception of "light" diatomics (e.g., H_2 or D_2) the $V \to V$ rates are expected to be much larger than $V \to R, T$ rates. The results are accordingly categorized into $V \to V$ and $V \to R, T$ processes in Table II.

In spite of the high endothermicity associated with the transfer of vibrational energy from CO to D_2, double-exponential decay of CO fluorescence was observed (see Fig. 1). Reduction of the data to specific rate information requires consideration of the following processes:
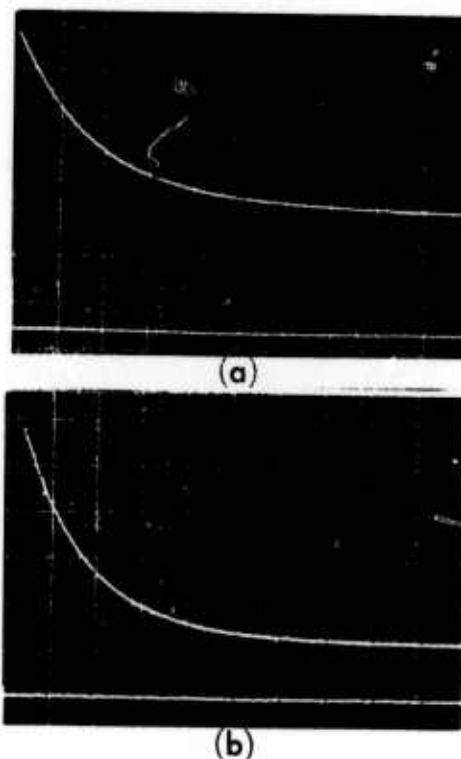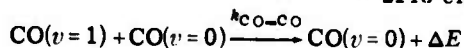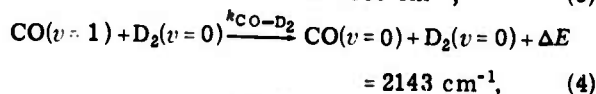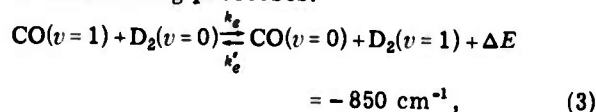
$$CO(v=1) + D_2(v=0) \underset{k_e'}{\overset{k_e}{\rightleftharpoons}} CO(v=0) + D_2(v=1) + \Delta E$$

$$= -850 \text{ cm}^{-1}, \tag{3}$$

$$CO(v=1) + D_2(v=0) \xrightarrow{k_{CO-D_2}} CO(v=0) + D_2(v=0) + \Delta E$$

$$= 2143 \text{ cm}^{-1}, \tag{4}$$

$$CO(v=1) + CO(v=0) \xrightarrow{k_{CO-CO}} CO(v=0) + \Delta E$$

FIG. 2. "Single shot" oscilloscope traces of CO fluorescence from two CO–N_2 samples. Listed pressures are in torr. $CO(v=1) + N_2 \rightleftharpoons CO + N_2(v=1) + \Delta E = -188$ cm^{-1}. (a) $P_{N_2} = 18.2$, $P_{CO} = 6.77$, $\tau_f = 156$ μsec, $\tau_s = 28$ msec, base line (500 μsec/cm). (b) $P_{N_2} = 61.0$, $P_{CO} = 7.95$, $\tau_f = 67$ μsec, $\tau_s = 26$ msec, base line (50 μsec/cm).

W. H. GREEN AND J. K. HANCOCK

TABLE II. CO–M relaxation data from singly relaxing mixtures.

	M	P_{CO}(torr)	P_M(torr)	τ(sec)	k(sec^{-1} torr^{-1})[a]
$V \rightarrow R,\ T$:	He	4.76	527	2.80(−3)[b]	0.68
		4.76	748	1.87(−3)	0.71
		5.93	391	3.58(−3)	0.71
					0.70 ±0.04, −0.08
	Ar	5.95	744	1.75(−2)	0.08
		7.95	310	2.65(−2)	0.12
					0.10 +0.04, −0.10
	H$_2$	1.07	257	2.70(−4)	14.14
		2.04	547	1.22(−4)	15.0
		11.5	370	1.86(−4)	14.5
		18.1	262	2.60(−4)	14.7
					14.6 ±1.2
$V \rightarrow V$:	O$_2$	23.0	257	1.34(−3)	2.90
		23.0	433	8.37(−4)	2.76
		3.5	630	6.10(−4)	2.60
					2.75 ±0.30
	Cl$_2$	4.26	548	7.57(−4)	2.41[c]
		4.21	516	8.30(−4)	2.33
					2.37 +0.20, −0.60
	NO	4.14	14.4	1.00(−4)	693
		5.07	52.4	2.73(−5)	699
					695 ±25
	CH$_4$	2.18	18.2	1.91(−4)	286
		2.70	61.0	5.40(−5)	307
		1.75	123	2.80(−5)	290
					293 ±14
	CF$_4$	5.76	5.74	2.61(−5)	6.67(3)
		10.35	1.70	9.26(−5)	6.35(3)
		2.05	7.18	2.38(−5)	5.85(3)
					(6.29 ±0.88)(3)
	SF$_6$	2.09	299	9.55(−5)	35.0
		5.67	199	1.43(−4)	35.0
					35.0 ±1.0

[a]$k_{CO–AB}$ has not been corrected for τ_{rad}=30 msec, however, in those cases where τ_{rad} is a significant factor, the error limits are expanded to cover the uncertainty.
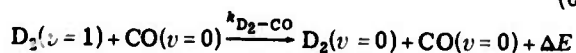[b]2.80(−3) = 2.80 ×10^{-3}.
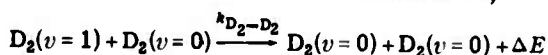[c]The lower error limit reflects the uncertainty of ≤200 ppm CO$_2$ impurity in the Cl$_2$ sample.

$$= 2143 \text{ cm}^{-1}, \qquad (5)$$

$$CO(v=1) \xrightarrow{k_{rad}} CO(v=0)+h\nu = 2143 \text{ cm}^{-1} \qquad (6)$$

$$D_2(v=1)+CO(v=0) \xrightarrow{k_{D_2–CO}} D_2(v=0)+CO(v=0)+\Delta E$$

$$= 2993 \text{ cm}^{-1}, \qquad (7)$$

$$D_2(v=1)+D_2(v=0) \xrightarrow{k_{D_2–D_2}} D_2(v=0)+D_2(v=0)+\Delta E$$
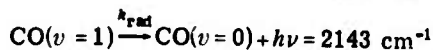
$$= 2993 \text{ cm}^{-1} . \qquad (8)$$

As depicted in Fig. 1, each mixture examined can yield three pieces of data: τ_f, the faster decay time; τ_s, the slower decay time; and S, the ratio of pre-exponential amplitude factors, C/D.

From an earlier paper[27] it can be shown that

$$a_1 = (\tau_s^{-1}+S\tau_f^{-1})/(1+S) = k_{CO–CO}P_{CO}$$
$$+ (ke+k_{CO–D_2})P_{D_2}+\tau_{rad}^{-1} \qquad (9)$$

and

$$b_2 = (\tau_f^{-1}+S\tau_s^{-1})/(1+S) = (ke'+k_{D_2–CO})P_{CO}+k_{D_2–D_2}P_{D_2}, \qquad (10)$$

where a_1 is the total rate of $CO(v=1)$ energy transfer represented in Eqs. (3)–(6), and b_2 is the corresponding rate for $D_2(v=1)$ shown in Eqs. (3), (7), and (8). For the first CO–D$_2$ mixture (see Table III), $a_1 = 2126$ sec^{-1}. Once again the term containing $k_{CO–CO}$ may be ignored and the small τ_{rad}^{-1} correc-

TABLE III. CO—D$_2$ and N$_2$ relaxation data.

	Mixture(torr)		τ_f(sec)	τ_s(sec)	S	ke(sec⁻¹·torr⁻¹)	k_{CO-D_2}(sec⁻¹·torr⁻¹)	$k_{D_2-D_2}$(sec⁻¹·torr⁻¹)
CO—D$_2$:	2.04	CO	3.95(−4)	2.75(−3)	4.35	3.04	0.45	0.63
	609	D$_2$						
	3.66	CO	3.80(−4)	3.32(−3)	2.26	$\frac{3.05}{3.05 \pm 0.10}$	$\frac{0.45}{0.45 \pm 0.15}$	$\frac{0.59}{0.61 \pm 0.15}$
	550	D$_2$						
CO—N$_2$	7.95	CO	7.20(−5)	2.65(−2)		172		
	61.0	N$_2$						
	310	Ar						
	6.77	CO	1.60(−4)	2.78(−2)		178		
	18.2	N$_2$						
	264	Ar						
	2.02	CO	2.02(−5)	6.60(−2)		173		
	281	N$_2$						
	79.0	Ar						
	3.15	CO	3.97(−5)	···		$\frac{175}{175 \pm 6}$		
	135	N$_2$						
	123	Ar						

tion is reflected in the final error limits. Therefore, Eq. (9) reduces to

$$(ke + k_{CO-D_2}) = 3.48 \text{ sec}^{-1} \cdot \text{torr}^{-1}. \quad (11)$$

Similarly, Eq. (10) yields $b_2 = 769$ sec⁻¹. At this point, separation of the $V \to V$ and $V-R$, T processes may be accomplished using the relation[27]

$$keke' = [S/(S+1)^2] (\tau_f^{-1} - \tau_s^{-1})^2/P_{CO} P_{D_2}$$
$$= 575 \text{ sec}^{-2} \cdot \text{torr}^{-2}, \quad (12)$$

and detailed balancing which provides $ke'/ke = e^{-\Delta E/kT}$. Solution of Eqs. (11) and (12) gives $ke = 3.05$ sec⁻¹ · torr⁻¹, $ke' = 189$ sec⁻¹ · torr⁻¹ and $k_{CO-D_2} = 0.45$ sec⁻¹ · torr⁻¹.

Recent measurements of Hopkins and Chen[28] have shown that $k_{D_2-He} = 0.63 \pm 0.7$ sec⁻¹ · torr⁻¹. It is reasonable to assume that $k_{D_2-CO} \le k_{D_2-He}$, and hence that $(ke' + k_{D_2-CO}) \simeq ke' = 189$ sec⁻¹ · torr⁻¹ and Eq. (10) produce $k_{D_2-D_2} = 0.63$ sec⁻¹ · torr⁻¹. The average values derived from two mixtures along with reasonable error limits are represented in Table III.

Reduction of the CO—N$_2$ experimental data is greatly simplified for it is known that the CO—N$_2$ rate processes corresponding to those represented for CO—D$_2$ in Eqs. (4)–(8) are all orders of magnitude smaller[11,29] than the $V \to V$ equilibration process,

$$CO(v=1) + N_2(v=0) \underset{ke'}{\overset{ke}{\rightleftharpoons}} CO(v=0) + N_2(v=1) + \Delta E$$
$$= -188 \text{ cm}^{-1}, \quad (13)$$

and may be neglected. Addition of Eqs. (9) and (10) gives

$$\tau_f^{-1} + \tau_s^{-1} = keP_{N_2} + ke'P_{CO}. \quad (14)$$

Typical "single-shot" oscilloscope traces of fluorescence from CO—N$_2$ mixtures are shown in Fig. 2; the experimental data for several CO—N$_2$ mixtures are contained in Table III.

DISCUSSION

CO $V \to R$, T Energy Transfer

The CO $V \to R$, T rates listed in Table IV are consistently 30%–40% faster than the early values reported by Millikan. Nevertheless, when one considers the substantial differences between the steady-state quenching and laser-fluorescence methods, this agreement is remarkably good.

The relatively large k_{CO-H_2} rate has been previously attributed to a nearly resonant $V \to R$ mechanism. Millikan and co-workers[30] have shown that para-H$_2$ is about twice as effective as ortho-H$_2$ in deactivating CO($v=1$). A postulate was forwarded that para-H$_2$ ($J=2$) undergoes near-resonant exchange with CO as represented by the following equation:

$$CO(v=1) + H_2(J=2) \underset{k_{VR}'}{\overset{k_{VR}}{\rightleftharpoons}} CO(v=0) + H_2(J=6) + \Delta E$$
$$\cong 88 \text{ cm}^{-1}, \quad (15)$$
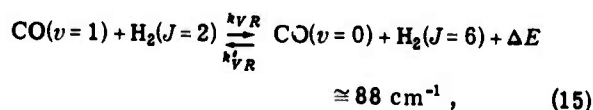
whereas ortho-H$_2$ lacks such a match with CO. A recent calculation of Sharma and Kern[31] lends direct support to the proposed mechanism.

On the other hand, the rotational degrees of freedom possessed by D$_2$, as well as its larger Lennard-Jones attractive potential,[32] apparently do not make it a more efficient $V \to R$, T quencher of

TABLE IV. $V \rightarrow R$, T rates from CO-additives mixtures.

Collision pair	Rate constant $\sec^{-1}$ torr^{-1}	Cross section[a] $\sigma(\text{Å})^2$	Z, collisions per[b] deactivation
$CO^\dagger$ + H$_2$	(14.6 ± 1.2)	$2.5(-5)$	$1.3(6)$
D$_2$	(0.45 ± 0.15)	$1.0(-6)$	$3.0(7)$
He	$(0.70 + 0.04, -0.08)$	$1.6(-6)$	$1.8(7)$
Ar	$(0.10 + 0.04, -0.10)$	$<5.1(-7)$	$>7.6(7)$
D$_2^\dagger$ + D$_2$	(0.61 ± 0.15)	$1.1(-6)$	$2.4(7)$

[a]Collision quenching cross sections can be calculated from $\sigma(\text{Å}^2) = 7.26 \times 10^{-8} kT^{1/2} \mu^{1/2}$, where k is the rate constant in $\sec^{-1} \cdot$ torr^{-1}, T is in degrees Kelvin and μ = the reduced mass in amu.

[b]Collisions per deactivation $Z = Z_{ab}/k$. The collision frequency $Z_{ab} = 4.32 \times 10^7 d_{AB}^2 T^{-1/2} \mu^{-1/2}$, where the collision diameter $d_{AB} = \frac{1}{2}(d_A + d_B)$ in angstroms. Hard sphere collision diameters were taken from Ref. 32 to be the following: 3.6 CO, 2.6 He, 3.4 Ar, 2.9 H$_2$, 2.9 D$_2$, 3.7 N$_2$, 3.2 NO, 4.4 A$_2$, 3.5 O$_2$, 3.8 CH$_4$, 4.7 CF$_4$, and 5.5 SF$_6$.

CO($v = 1$) than is He (see Table IV). Evidence that He is at least as effective as D$_2$ in quenching CO was also determined by Miller and Millikan,[33] who found that data ranging from near room temperature down to 110 °K were nearly superimposable for the two additives. Shock tube studies show an analogous trend at high temperatures.[34] Though the role of rotation is unclear, relaxation data are becoming sufficiently extensive that theoretical models may be put to the test.

It should be noted that the experimental trend discussed above qualitatively agrees with that observed for the relaxation of D$_2$($v = 1$) in shock tube studies carried out by Bird and Breshears.[35] Over the 1400–3500 °K temperature range studied, D$_2$ was a *less* effective quencher of D$_2$($v = 1$) than was ^{4}He. Data to the contrary also exist, however. For example, Hopkins and Chen[36] have reported the opposite behavior from room temperature laser-fluorescence measurements on HCl–D$_2$–He mixtures. The $k_{D_2-D_2}$ value reported by Hopkins and Chen[28,36] is about 30% larger than the rate determined from the present study. It would appear that a careful study of $k_{D_2-D_2}$ and k_{D_2-He} from room temperature to 1400 °K would be worthwhile.
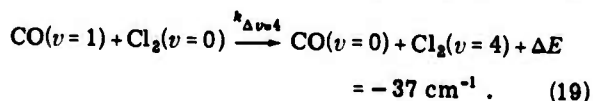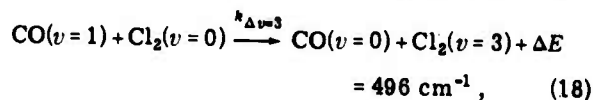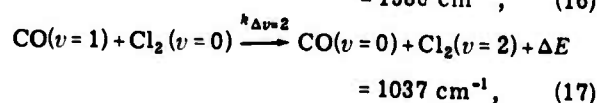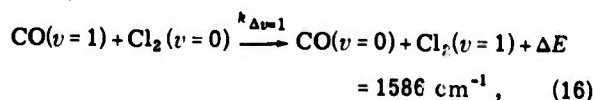
Accurate assessment of either the CO–CO or CO–Ar $V \rightarrow T$ rates by the present technique would require sample pressures well above 1 atm to assure that collisional deactivation could compete favorably with the CO radiative decay and that effects of radiation trapping could be ignored. The CO–Ar rate of 0.10 $\sec^{-1} \cdot$ torr^{-1} in Table IV is an upper limit only. In all probability, $k_{CO-Ar} < k_{CO-CO} \leq 1.9 \pm 0.6 \times 10^{-3} \sec^{-1} \cdot$ torr^{-1}.[16]

CO $V \rightarrow V$ Transfer to Diatomics

Table V summarizes the CO–AB $V \rightarrow V$ data obtained in the present investigation. The k_{CO-N_2}

rate is in excellent agreement with Stephenson's results[19] and in very good agreement with the value of Zittel and Moore,[8] whereas the early value of Green and Hancock[7] now appears to have been 25% too low. The k_{CO-NO} rate agrees very well with that of Basco *et al.*[10] obtained from flash kinetic spectroscopy, as well as the recent value of Stephenson.[20] Our value for k_{CO-O_2} is over an order of magnitude less than found in the 376 °K ultrasonics measurement of Bauer and Roesler,[12] is ~30% larger than the result from Millikan's steady-state experiment, and is within 5% of Stephenson's value.

For CO $\rightarrow$ D$_2$ and CO $\rightarrow$ Cl$_2$ transfer, the measured rates are relatively much faster than would be expected solely from considerations of fundamental energy defect. The large rotational spacing of D$_2$ most likely allows some of the large CO($v = 1$) and D$_2$($v = 1$) band center mismatch (850 cm^{-1}) to be absorbed through ΔJ changes with a resulting enhancement in energy transfer. On the other hand, the Cl$_2$ molecule presents a situation where Cl$_2$ ($\Delta v = 2, 3$, and 4) transfers are much more resonant than Cl$_2(\Delta v = 1)$ as is depicted by the following equations:

$$CO(v=1) + Cl_2(v=0) \xrightarrow{k_{\Delta v=1}} CO(v=0) + Cl_2(v=1) + \Delta E$$
$$= 1586 \text{ cm}^{-1}, \quad (16)$$

$$CO(v=1) + Cl_2(v=0) \xrightarrow{k_{\Delta v=2}} CO(v=0) + Cl_2(v=2) + \Delta E$$
$$= 1037 \text{ cm}^{-1}, \quad (17)$$

$$CO(v=1) + Cl_2(v=0) \xrightarrow{k_{\Delta v=3}} CO(v=0) + Cl_2(v=3) + \Delta E$$
$$= 496 \text{ cm}^{-1}, \quad (18)$$

$$CO(v=1) + Cl_2(v=0) \xrightarrow{k_{\Delta v=4}} CO(v=0) + Cl_2(v=4) + \Delta E$$
$$= -37 \text{ cm}^{-1}. \quad (19)$$

While it is true that, other things being equal ener-

TABLE V. $V \rightarrow V$ rates from CO-additive mixtures.

Collision pair	Energy defect (cm^{-1})	Rate constant sec^{-1}·torr^{-1}	Cross section $\sigma(\text{Å})^2$	Z, collisions per deactivation
CO† + N$_2$	−188	175 ± 6	8.2(−4)	5.1(4)
+ NO	267	695 ±25	3.3(−3)	1.1(4)
+ O$_2$	588	2.75 ± 0.30	1.3(−5)	3.0(6)
+ D$_2$	−850	3.05 ± 0.10	7.1(−6)	4.6(6)
+ Cl$_2$	$\begin{bmatrix} 1586 \\ 1037 \\ 496 \\ -37 \end{bmatrix}^a$	2.4 +0.20, −0.60	1.3(−5)	3.8(6)
CO† + CH$_4$	837^b(ν_4)	293 ±14	1.2(−3)	3.7(4)
+ CF$_4$	−43^b($\nu_1 + \nu_3$) 862 (ν_3)	(6.29 ±0.88)(3)	1.6(−5)	1.5(3)
+ SF$_6$	~430^b($\nu_1 + \nu_3$) ~1200 (ν_3)	35.0 ±1.0	2.1(−4)	3.1(5)

^{a}Energy defects are calculated for Cl$_2$($\Delta v \leq 4$) from the data in G. Herzberg, *Molecular Spectra and Molecular Structure I. Diatomic Molecules* (Prentice-Hall, New York, 1939), p. 485.

^{b}The actual vibrational states receiving energy in polyatomic additives are not known. The tabulated energy defects assume transfer to levels chosen on the basis of ir activity and degree of resonance.

gy transfer probabilities should decrease as the number of vibrational quanta changed during a collision increases, it is also true that the probability should increase approximately exponentially with decreasing energy defect. Other investigations have produced strong evidence of multiquantum transfer in somewhat similar situations where overtones were much more nearly resonant than fundamentals.[7,9,37] Whether or not multiquantum transfer to Cl$_2$ occurs can not be determined by the present experiment, but the unusually fast $k_{\text{CO}-\text{Cl}_2}$ may indicate that it does.

Figure 3 is a semilog plot of $V \rightarrow V$ energy transfer probability versus T for the data obtained herein and the shock tube data of Sato *et al.*[29] on the CO–NO, N$_2$, O$_2$, and D$_2$ collision pairs. Interpolation between the room temperature laser-fluorescence data and the higher temperature shock tube data can provide a rather complete picture of these $V \rightarrow V$ processes over a wide temperature range.

CO $V \rightarrow V$ Transfer to Polyatomics

Experimental data for CO–CH$_4$, CF$_4$, and SF$_6$ mixtures are contained in Table V. The rate $k_{\text{CO}-\text{CH}_4} = 293$ sec^{-1}·torr^{-1} is somewhat less than the 340 and 400 sec^{-1}·torr^{-1} values determined by

Millikan[38] and Kovacs,[39] respectively, but still seems too large to reflect a pure $V \rightarrow R, T$ mechanism. In principle, CO can transfer a vibrational quantum to any of the CH$_4$ fundamental vibrations. One would expect the $V \rightarrow V$ probability to depend primarily upon the degree of resonance and the magnitude of the transition matrix elements. CH$_4$ has infrared active modes at 1306 and 3020 cm^{-1} [40]

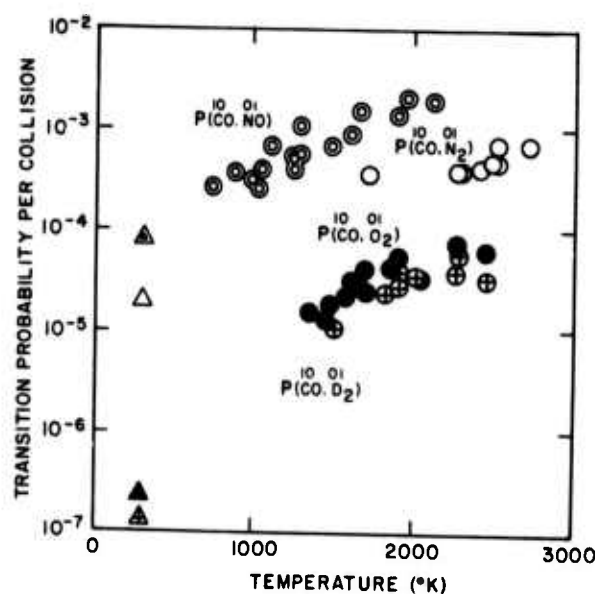FIG. 3. $V \rightarrow V$ energy transfer probabilities versus temperature for CO($v=1$) + $AB(v=0) \rightleftarrows$ CO($v=0$) + $AB(v=1$). $\odot$, $\triangle$ = NO; O, $\triangle$ = N$_2$; •, ▲ = O$_2$; and, •, ⊕ = D$_2$; circles = shock tube data of Ref. 29, triangles = fluorescence data of present study.

and infrared inactive modes at 2914 and 1526 cm^{-1}. On this basis the 1306 cm^{-1} mode is a likely candidate; nevertheless, direct evidence as to which vibrational mode(s) is involved is lacking and transfer to combination bands cannot be ruled out.

Because of its greater mass, larger moment of inertia, and greater mismatch of fundamental levels with CO, one would expect *a priori* that CF_4 should be a *less* efficient quencher of CO than is CH_4. In fact, CF_4 relaxes $CO(v=1)$ over 20 times faster than does CH_4. If transfer to the closest fundamental ($\nu_3 = 1281$ cm^{-1}) is ruled out, energy match and infrared activity point to the $(\nu_1 + \nu_3)CF_4$ combination band at 2180 cm^{-1} as the probable recipient of energy from CO. The CF_4 result tends to explain the experiment of Lin[41] in which very rapid quenching of laser emission from CO $(6 \leq v \leq 12)$ was observed upon the addition of CF_4. Conversely, it was noted by Lin that SF_6 had little effect upon laser output—an observation which is consistent with the moderately slow rate, $k_{CO-SF_6} = 35$ sec^{-1} $\cdot torr^{-1}$, measured in the present study.

SUMMARY

The frequency-doubled CO_2 laser constitutes an ideal source with which CO(or NO^{20}) energy transfer rates may be measured *directly*, by a technique that is characterized by high precision and inherent simplicity. Extension to the study of high and low temperature samples is straightforward since coincidental overlap exists for both the $R(2)$ and $P(14)$ CO transitions and this in turn assures an adequate Boltzmann population of the specific level being pumped. In particular, accurate relaxation measurements at the low operational temperatures associated with current CO lasers are now feasible.

The $CO(v=1)$ $V \to V$ processes, if anything, are much faster than expected. Unusually large cross sections found for $CO \to CF_4$ and $CO \to Cl_2$ appear to be explainable as transfer to nearly resonant combination or overtone levels rather than to nonresonant fundamental levels.

ACKNOWLEDGMENTS

[1] R. C. Millikan, Phys. Rev. Lett. **8**, 253 (1962); J. Chem. Phys. **38**, 2855 (1963).

[2] L. O. Hocker, M. A. Kovacs, C. K. Rhodes, G. W. Flynn, and A. Javan, Phys. Rev. Lett. **17**, 233 (1966).

[3] J. T. Yardley and C. B. Moore, J. Chem. Phys. **45**, 1066 (1966); see also C. B. Moore, in *Fluorescence*, edited by G. G. Guilbault (Dekker, New York, 1967), p.133.

[4] For example, see H. L. Chen and C. B. Moore, J. Chem. Phys. **54**, 4072 (1971); J. Chem. Phys. **54**, 4081 (1971); J. R. Airey and S. F. Fried, Chem. Phys. Lett. **8**, 23 (1971); H. L. Chen, J. Chem. Phys. **55**, 5551 (1971); J. Chem. Phys. **55**, 5557 (1971); and J. K. Hancock and W. H. Green, J. Chem. Phys. **56**, 2474 (1972).

[5] However, timed Q-switching has produced $CO(v = 1 \to v = 0)$ lines: D. W. Gregg and S. J. Thomas, J. Appl. Phys. 39, 4399 (1968); continuous laser emission from the CO $(v = 2 \to v = 0)$ first overtone transition has been reported by F. G. Sadie, P. A. Buger, and D. G. Malan, J. Appl. Phys. 43, 2906 (1972); and very recently N. Djeu of NRL has succeeded in producing $CO(v = 1 \to v = 0)$ laser emission [Appl. Phys. Lett. 23, 309 (1973)].

[6] C. B. Moore, Adv. Chem. Phys. **23**, 41 (1973).

[7] W. H. Green and J. K. Hancock, IEEE J. Quantum Electron. QE-9, 50 (1973).

[8] P. F. Zittel and C. B. Moore, Appl. Phys. Lett. **21**, 81 (1972).

[9] P. F. Zittel and C. B. Moore, J. Chem. Phys. **58**, 2922 (1973).

[10] R. J. Donovan and D. Husain, Trans. Faraday Soc. **63**, 2879 (1967); N. Basco, A. B. Callear, and R. G. W. Norrish, Proc. R. Soc. A **60**, 459 (1961); and Proc. R. Soc. A **269**, 180 (1962).

[11] W. J. Hooker and R. C. Millikan, J. Chem. Phys. **38**, 214 (1963).

[12] H. J. Bauer and H. Roesler, *Molecular Relaxation Processes* (Academic, New York, 1966), p. 245; H. J. Bauer and J. Roesler, Z. Naturforsch. A **19**, 656 (1964).

[13] W. E. Woodmansee and J. C. Decius, J. Chem. Phys. **36**, 1831 (1962); M. G. Ferguson and A. W. Read, Trans. Faraday Soc. **61**, 1559 (1965).

[14] G. Hancock and I. W. M. Smith, Appl. Opt. **10**, 1827 (1971).

[15] C. Wittig and I. W. M. Smith, Chem. Phys. Lett. **16**, 292 (1973); H.T. Powell (private communication).

[16] M. A. Kovacs and M. E. Mack, Appl. Phys. Lett. **20**, 487 (1972).

[17] H. Dubost, L. Abouaf-Marguin, and F. Legay, Phys. Rev. Lett. **29**, 145 (1972).

[18] J. K. Hancock and W. H. Green, "The Application of a Frequency-Doubled CO_2 Laser to Energy Transfer Measurements in CO," presented at the 8th Middle Atlantic Regional Meeting (MARM) of the American Chemical Society, Washington, D. C., Jan. 17, 1973.

[19] J. C. Stephenson, Appl. Phys. Lett. 22, 576 (1973).

[20] J. C. Stephenson, J. Chem. Phys. 59, 1523 (1973).

[21] E. g. see C. K. N. Patel, Phys. Rev. Lett. **8**, 62 (1965); J. D. Taynai, R. Targ, and W. B. Tiffany, IEEE J. Quantum Electron. QE-7, 412 (1971); and W. B. Gandrud and R. L. Abrams, Appl. Phys. Lett. 17, 302 (1970).

[22] T. Y. Chang, Opt. Commun. 2, 77 (1970).

[23] IUPAC, *Tables of Wavenumbers for the Calibration of Infrared Spectrometers* (Butterworth, Washington, D.C., 1961)

[24] E. g. See B. M. Hopkins and H. L. Chen, J. Chem. Phys. 57, 3816 (1972).

[25] D. W. Bresnears, Chem. Phys. Lett. 20, 429 (1973).

[26] See R. A. Toth, R. H. Hunt, and E. K. Plyler, J. Mol. Spectrosc. 32, 85 (1969), and references cited therein.

[27] J. K. Hancock and W. H. Green, J. Chem. Phys. 57, 4515 (1972).

[28] B. M. Hopkins and H. L. Chen, J. Chem. Phys. **58**, 1277

(1973).

[29]Y. Sato, S. Tsuchiya, and K. Kuratani, J. Chem. Phys. 50, 1911 (1969); likewise, k_{CO-Ar} and k_{N_2-Ar} are believed to be negligibly small.

[30]E. g. R. C. Millikan and L. A. Osburg, J. Chem. Phys. 41, 2196 (1964).

[31]R. D. Sharma and C. W. Kern, J. Chem. Phys. 55, 1171 (1971).

[32]J. O. Hirschfelder, C. F. Curtiss, and R. B. Bird, *Molecular Theory of Gases and Liquids* (Wiley, New York, 1954), p. 1110.

[33]D. J. Miller and R. C. Millikan, J. Chem. Phys. 53, 3384 (1970); and D. J. Miller, Ph.D. thesis, University of Southern California at Santa Barbara, December 1972.

[34]R. C. Millikan, J. Chem. Phys. 40, 2594 (1964); D. R. White, J. Chem. Phys. 45, 1257 (1966).

[35]P. F. Bird and W. D. Breshears, Chem. Phys. Lett. 13, 529 (1972).

[36]B. M. Hopkins and H. L. Chen, J. Chem. Phys. 57, 3161 (1972).

[37]J. Ahl and T. A. Cool, J. Chem. Phys. 58, 5540 (1973).

[38]R. C. Millikan, J. Chem. Phys. 43, 1439 (1965).

[39]M. A. Kovacs, J. Chem. Phys. 58, 4704 (1973).

[40]G. Herzberg, *Infrared and Raman Spectra* (van Nostrand, New York, 1964), p. 307.

[41]M. C. Lin (private communication).

APPENDIX C

A LARGE APERTURE HIGH EXTINCTION RATIO FARADAY ROTATOR ISOLATOR*

O.C. Barr, J.M. McMahon and J.B. Trenholme[†]

Interaction Physics Branch
Optical Sciences Division

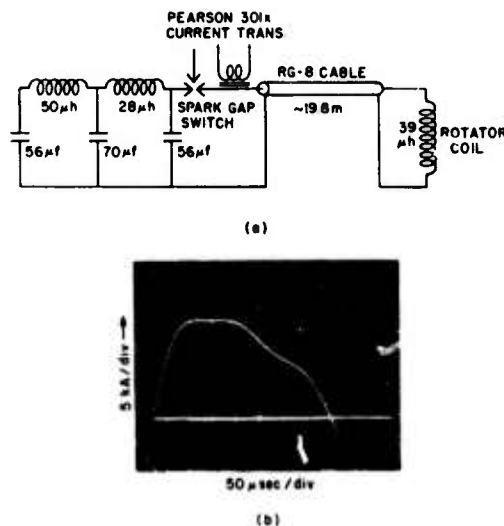Naval Research Laboratory
Washington, D.C. 20375

C-1
(Page C-2 blank)

Fig. 1. (a) Driving circuit for the Faraday rotator. The 39-μH rotator solenoid consisted of 41 turns of 6.35- × 12.7-mm rectangular cross-section copper wire wound on a 9-cm-diameter form 29 cm long. (b) Current waveform produced by the driving circuit as measured by the Pearson 301 X current transformer and a Tektronix 556 oscilliscope. 21.5 kA was required for 45° rotation.

Fig. 2. Measured extinction ratio versus angle of rotation. (— — —) shows a calculation for an ideal case while (———) and (- - - -) show calculations for 37-dB and 35-dB extinction systems, respectively.

A Large-Aperture High-Extinction-Ratio Faraday-Rotator Isolator

O. C. BARR, J. M. McMAHON, AND J. B. TRENHOLME

Abstract—A 45° Faraday rotator has been built at the Naval Research Laboratory. This rotator is designed for use with a short-pulse high-peak-power laser, and it has demonstrated an extinction ratio in excess of 35 dB.

Laser-heated pellet approaches to controlled fusion require that kilojoule-level laser intensities be directed on a target in a pulse of less than a nanosecond duration. This places severe constraints on the generating laser in order to avoid self-focusing. Additionally, the target will reflect some fraction of the incident intensity, and unless isolation is incorporated in the amplifier chain this reflected energy can be amplified to disastrously high levels.

45°-Faraday-rotator isolators appear to be the only practical isolation device for the large apertures required of kilojoule-level Nd: glass lasers (15–25 cm), as the material is not available for
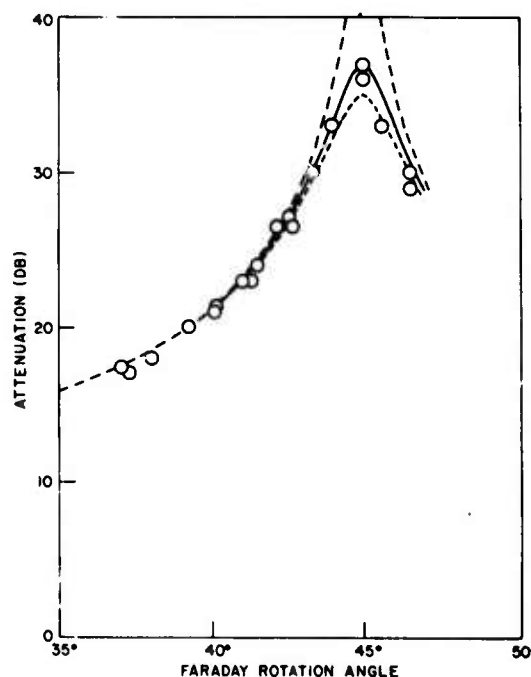
Pockel's cells in these sizes and stimulated processes may occur in Kerr cells. Conventional approaches have, however, led to Faraday-rotator isolators with disappointingly low extinction ratios (e.g., 16–17 dB for the CGE FR-70 isolator [1]) which severely impact systems design [2].

We have accordingly looked at the problems which limit the extinction ratio for Faraday-rotator isolators. The fundamental limitation is the color dispersion of the Verdet constant across the gain–bandwidth of Nd: glass. For typical glasses this limits the achievable extinction ratio to 35–40 dB [3]. The glass must also be very well annealed and strain free to be compatible with extinction ratios in the same range.

The magnetic field must have 1-percent uniformity to achieve 40-dB extinction across the system aperture. This degree of field uniformity can be achieved most easily by using a rotator coil which is much longer than the length of the rotator glass.

The fraction of the light which is twice reflected at the glass–air interface will emerge rotated 135° relative to the backward-traveling beam and will pass the polarizer [4]. For a high-index glass, such as Owens-Illinois EY-1 terbium glass, this component will be weaker than the incident intensity by ~26 dB. It can be eliminated by anti-reflection coating on one or both surfaces of the rotator glass, but in fact is not a significant system limitation since the next Faraday rotator in the system will reject it along with any other cross-polarized component of the back reflection.

The basic NRL design is an 8-cm-aperture Faraday rotato which uses a 2-cm-thick piece of Owens-Illinois EY-1 glass in a 41-turn solenoid 29 cm long. This coil is driven by a resistivity-damped three-mesh pulse-forming network to produce a 34-kG field with less than a 1-percent temporal variation over 95 μs. This enables the laser electronics to check that the Faraday rotators are operating properly before a laser pulse is generated.

The solenoid design was similar to that employed by the National Magnet Laboratory [5], [6] and used fiberglass construction to achieve adequate strength. Fig. 1(a) shows the solenoid driving network and Fig. 1(b) shows the current waveform obtained with this network.

The extinction ratio was checked using a 900-ps pulse generated by a mode-locked oscillator with the Faraday rotator between crossed polarizers. The signal was spatially filtered to reject the multiply reflected component. Fig. 2 shows the results of these measurements. The best fit to the data was attained for an extinction ratio of 36 ± 1 dB.

These experiments are quite encouraging from a systems standpoint, in that a design has been validated suitable for use in the proposed 10^6-J laser system at the Lawrence Livermore Laboratory. Several engineering improvements on the present design appear possible. The PFN was used to insure that a valid current measurement could be made with no interference from noise. In fact the noise level is low enough that a valid dI/dt measurement can be used on the current rise and a single-mesh capacitor bank could be used to reduce the bank size by a factor of 4. The strength of the fiberglass coil design can also be improved to permit the use of thinner plates of rotator glass at higher field strengths (within optical polishing constraints) which may be necessary for very large apertures, reducing the volume of high Verdet constant glass required.

REFERENCES

[1] Hadron, Inc., data sheet FR-70.
[2] J. B. Trenholme "The design of a large laser system for fusion," presented at the 1973 IEEE Conf. Laser Engineering and Applications, Washington, D.C., May 30–June 1, 1973.
[3] J. F. Holzrichter "Faraday rotation in EY-1 glass," Naval Research Laboratory, Washington, D.C., NRL Memo. Rep. 2510, Sept. 1973.
[4] J. McLeod, Los Alamos Scientific Laboratory, private communication.
[5] D. B. Montgomery, Solenoid Magnet Design. New York: Wiley, 1969.
[6] Y. Iwasa, Bitter National Magnet Laboratory, private communications.

APPENDIX D

GLASS LASER SYSTEM USED ROUTINELY FOR TARGET IRRADIATION

J.M. McMahon and O.C. Barr

Naval Research Laboratory
Washington, D.C. 20375

INTRODUCTION

The design of a neodymium glass laser system for irradiation of
targets of $10^{11} - 10^{12}$ watt pulses in a high brightness beam requires
simultaneous solution of a number of technical problems. These
problems can be separated into two areas relating to self focusing
and to target and interstage isolation in the system.

The desired output powers for lasers used in fusion research are
60 - 80 db over the critical power ($\approx$ 1 MW) for self focusing, making
self focusing a severe limitation on their operation. Since the
mechanisms causing self focusing for subnanosecond pulses appear to have
picosecond response times, any temporal structure on the beam will lead
to catastrophic self focusing at abnormally low average intensity
levels precluding successful operation. Other dramatic manifesta-
tions of self focusing include beam decollimation due to self focusing
of intensity variations, non-linear wavefront distortion, and linewidth
broadening due to self phase modulation.

Backscatter from the target, collimated into the laser, can be
amplified backwards until some early stage is catastrophically damaged.
Self focusing damage is easily generated by this back reflected pulse
since it is converging and is of uncertain spatial and temporal
character. A useful high power system must be adequately isolated
from such backscatter. Additionally, the isolation system serves to
minimize uncontrolled preheating of the target (prelase) and enhance
the peak to background ratio for the main pulse. System requirements
include high reliability, a fail safe nature, and minimum cost per
shot.

AMPLIFIER CHAIN CONFIGURATION

The basic engineering problem with high peak power solid state
laser systems is how to maximize the peak power generated while
preserving adequate beam quality and reliability. The major difficulty

with subnanosecond systems stems from the fact that solid state laser
materials have a nonlinear index of refraction whose magnitude depends
on the intensity of the light field in the material; that is,

$$n = n_o + n_2 E^2 \qquad (2)$$

where n_o is the ordinary index of refraction and E is the electric
field strength of the light field. The coefficient n_2 is a measure
of the effect of the light field on the internal fields in the material.
Kelley (who first discovered the relation in Eqn. 1) showed that this
effect would cause focusing of a laser beam because the index change
convoluted with the beam intensity profile will cause refraction of the
light rays towards the region of highest intensity.[1]

There are a number of possible mechanisms which can give self
focusing but in solids on subnanosecond time scales molecules are
unable to move (electrostriction) or rotate (rotational relaxation);
thus the only effect that concerns us is distortion of the electronic
field in the material by the strong applied laser field (Kerr effect).
This effect can be expected to have a very fast time response and in
fact measurements of n_2 with pulses between 10^{-11} and 10^{-9} seconds in
duration indicate that n_2 is essentially constant.[2,3]

This result has a very important consequence; a limitation on the
peak power density which will propagate without damage. A structure
capable of generating 1000 joules in 10^{-9} sec can generate no more than
1 J in 10^{-12} sec. There is therefore a very strong premium on designing
a system to maximize the power that can be generated from a given
aperture.

There are several factors which must enter into such an approach.
The first is that the pulse being amplified must be temporally smooth
as self focusing will follow any intensity structure on the pulse.
This is equivalent to saying that the optimum pulse is one whose time
duration if the Fourier transform of its bandwidth. In our system
this is achieved by using a mode locked Nd:YAG oscillator with internal
Fabry-Perot etalons to narrow the bandwidth (increase the pulsewidth)
to a desired value.

The first order effect of the nonlinear index of refraction is to
cause the solid state material to act as a positive lens. This can
be negated by diverging the basic beam such that the beam does not
collapse. In practice, this does not however solve the self focusing
problem since spatial structure on the beam can also self-focus.
This has in fact proven to be the most difficult problem to control

D-2

and it has recently been shown by Marberger[4] that index inhomo-
genetics in laser materials will cause intensity variations strong
enough to preclude a general solution to this problem for intensities
much in excess of 10^{10} W/cm.

Several approaches have been investigated at NRL and the Lawrence
Livermore Laboratory for minimizing spatial intensity fluctuations to
allow intensities on the order of 10^{10} W/cm^2 to be generated without
damage or beam breakup. The master oscillator must operate in the TEM_{oo}
(Gaussian) mode as correction of wavefront distortions becomes very
difficult for beams without azimuthal symmetry. The Gaussian
distribution is not optimal for amplification since the intensity
falls off very slowly in the wings and aperture diffraction of the
wings causes Fresnel fringes and downstream self focusing damage. The
approach we have followed is to modify the mode pattern to eliminate
the wings of the Gaussian. This is done by truncating the mode after
the oscillator at the e^{-4} intensity points and then truncating at the
first dark ring in the Airy disc in the far field. This procedure
results in a center lobe which smoothly goes to zero inside the system
aperture. The spatial intensity fluctuations on the center lobe due
to this procedure are on the order of 1%.[5] At LLL, Speck and
co-workers have investigated the use of saturable absorbers to suppress
the wings of the Gaussian by preferentially attenuating the weaker
regions of the beam and this procedure also seems to give very reason-
able results.[6]

The next order of problem which must be solved is staging of the
laser amplifiers to minimize system damage and wavefront distortion.
The key to this aspect of the problem comes in noting that the net
path length change through the amplifiers.

$$\Delta n(r) \approx kn_2 \int_0^L P(\ell, r) \, d\ell, \qquad (2)$$

and that a minimum distortion solution consists of minimizing the
integral. If we ignore saturation of the amplifiers for the moment
there is also a requirement that the path length be long enough to
amplify to the desired level, i.e.

$$L \approx \frac{1}{\alpha} \ell n \left(\frac{I_f}{I_o} \right) \qquad (3)$$

where α is the gain per unit length.

Our approach to this aspect of the problem has been to maximize α at each stage and to minimize the length over which $P(\ell,r)$ is in fact appreciable. This has been done by using Nd:YAG preamplifiers ($\alpha \sim .3$ cm^{-1}) to the size where it was necessary to use glass amplifiers ($\alpha \sim .1$ cm^{-1}) and then to use disc amplifiers ($\alpha \sim .08$ cm^{-1}) at the point where the unfavorable surface area to volume ratio of large rods decreased the pumping to the point where a lower gain resulted than is available from disc amplifiers.

The staging was carried another step in that saturation will result in a spatial profile which will approach a constant value across the beam center and roll off smoothly on the sides. This can be tailored somewhat to minimize transient wavefront distortion which will otherwise result in the focus of a beam at high intensity differing from the focus at low intensity. It should be emphasized that our system represents an engineering approach to the problem and that further refinements are being made after testing and evaluation on a continuing basis. In this spirit we present our experience on damage to the Owens-Illinois neodymium glass rods used in the system. The useful life is not the number of shots until filaments can first be seen but rather the number of shots before wavefront distortion (as determined by a shearing interferometer) occurs on an appreciable scale.

INTENSITY	LIFETIME
2×10^9 W/cm^2	∞
4×10^9 W/cm^2	~ 3000
$8 - 10 \times 10^9$ W/cm^2	~ 500
20×10^9 W/cm^2	< 10

In many cases the damage to the final rod amplifier has been caused by Fresnel diffraction around dust on optical surfaces, fringes due to misaligned polarizing prisms, etc. In principle this can be eliminated; in practice it is difficult to routinely operate in an ideal state; it is perhaps better to view the last entry in Table I as noting the tenuous stability of operation at these levels and also as an indication of the economics of operation of such a system.

Our experience with disc amplifiers has been somewhat different. A disc amplifier has many exposed surfaces and it is difficult to keep them clean; however, there is a relatively large ratio of path length in air to path length in the laser glass. The result is that at worst a beam emerges which has Fresnel patterns of the surface damage superimposed but we have not as yet seen any self focusing damage at intensity levels up through the highest in Table I.

We are currently working on clean, sealed disc laser geometries which will hopefully solve the surface problems; the initial indications are that these appear quite feasible, from an engineering standpoint, with a sacrifice of perhaps 10% in efficiency compared to the most optimum pumping geometry.

SYSTEM ISOLATION

An isolation system which effectively decouples the amplifiers in the laser system is required for a number of reasons. Stability of the amplifier chain will require some interstage isolation since the small signal gain of the amplifier cascade may approach 80 - 90 db. Unisolated amplifier cascades with gains in excess of 60 db tend to go into self oscillation. This not only reduces the gain for the main pulse, it also may preirradiate the target.

With targets of low thermal mass, preheating due to the fluorescence of the amplifiers as well as prepulsing by pulses generated prior to the gated pulse must be minimized. The latter can be achieved by a series of Pockel's cell gates each of which will suppress the background pulse train by 25 - 30 db. The former is a bit more difficult in that some fraction of the amplifier fluorescence will always heat the target. The main elements of a satisfactory solution to this problem are: elimination of parasitic oscillation in the amplifier chain by interstage isolation, a long path length between the last amplifier and the target to minimize the solid angle subtended by focusing lens and the use of the largest 1/F number lens allowable to achieve the desired spot size.

Reflection of the main pulse from the target plasma poses the most serious isolation problem. There appear to be two types of mechanisms which cause the observed backscatter. Laser light incident on the critical density region in the plasma ($n_c \sim 10^{21}$ cm^{-3} at 1.06 μ) will be reflected. The backscattered light will have a similar spectral character to the outgoing laser light but may be Doppler-shifted a few Angstroms by motion of the critical density region[7]. Stimulated processes analogous to stimulated Brillouin or Raman scattering may also occur. In the case of Brillouin scattering, many orders of Stokes and anti-Stokes components may be generated on either side of the laser spectrum within the gain bandwidth of the laser. At NRL we have observed total backscatter of $\sim$ 10% due to both of these mechanisms.

This backscattered signal can be amplified through the amplifier chain in reverse and in a few stages can reach a power density where it catastrophically self focuses. An isolation system must prevent this from happening and must suppress the intensity of any back reflected pulse to a safe level at each point in the amplifier train. The safe

level will in fact be much lower than the outgoing energy at that point since the reflected pulse does not have a carefully tailored spatial shape and may also have strong temporal modulation. A balanced system of Faraday rotators, Pockel's cells and polarizers are used at NRL to suppress the backreflected pulse at each stage to nominal safe levels, usually two to ten times less than the outgoing level at the same stage.

A Pockel's cell is used to gate out a single pulse from the mode locked pulse train with a peak to background ratio of 33 ± 1 db. A second Pockel's cell is used as a back reflection isolator and also to suppress the background by an additional 28 ± 1 db. Both Pockel's cells are fabricated such that they are part of a 50 Ω transmission line[8].

While a gated Pockel's cell attenuates both planes of polarization of the reflected light, a Faraday rotator-polarizer combination only attenuates one plane of polarization. That is, the output rotator rejects light polarized in the same plane as the outgoing pulse, the next rotator rejects any cross-polarized component and so on.

A standard 8 cm aperture, 45° Faraday rotator has been designed and is used at all points of greater than 3 cm aperture requiring an isolation element because large aperture Pockel's cells have higher losses than Faraday rotators and it is hard to obtain large high quality crystals. The rotators consists of a 2 cm thick, 8 cm diameter disc of Owens-Illinois EY-1 terbium glass centered in 29 cm long 9 cm ID pulsed solenoid. A 34 kG field is maintained constant (± 1%) for > 90 μsec by a 39 kJ, 3 mesh pulse forming network. This allows adequate time to abort the outgoing pulse in case of a rotator malfunction. Field uniformity within the rotator glass has been optically measured to be better than ±½% over the entire aperture, adequate for 40 db extinction between perfect polarizers.

The driving circuit and current waveform for the two rotators installed in the system are shown in Fig. 1. An extinction ratio of 36 ± 1 db has been obtained with these devices[9]. Since the variation of the Verdet constant across the gain bandwidth of neodymium glass places a limit of 35 db on the extinction ratio for back reflected light[10], this represents an adequate solution to the problem. It should be noted that there is a component doubly reflected in the rotator glass which is 26 db weaker than the main component which is rejected by the next rotator[11].

Each of these active elements requires polarizers to reject back reflected energy. The classical solution, i.e., air-spaced calcite glan polarizers has been found to be of marginal utility for several reasons. It is difficult to obtain large calcite prisms and addition-

ally a higher coherent diverging wavefront will be sheared by the interface which will produce a superimposed linear fringe pattern on the beam.

Presently thin film polarizing coatings which have a 20 db extinction ratios for one plane of polarization and 95% transmission for the other plane of polarization on substrates of BK-7 are used throughout the system at points where the energy density in the beam is ≤ 1 J/cm^2.* These coatings have been found to damage in 30 - 50 shots at ≈ 2 J/cm^2 but have shown no degradation over 1000 shots at the lower energy density.

Two 7 cm aperture fanned and wedged stacked plate polarizers have been designed and are used at locations where the energy density exceeds 1 J/cm^2. The 12 plate polarizer exhibits 20 db rejection and 94% transmission while a second with six plates achieved 10 db and 95% transmission. The plates are BK-7, wedged 1°, and are fanned for angles of incidence of 1 - 2° greater than Brewster's angle to minimize the number of plates. The polarizers are sealed to eliminate daily cleaning of the plates.

OPERATING EXPERIENCE

The laser system in use at NRL has evolved over the past year. The mode locked oscillator, gate and Nd:YAG preamplifiers are shown in Fig. 2. A basic system, shown in Fig. 3, consisting of glass rod amplifier stages only, was used until EY-1 Faraday rotator glass became available. This rod system produced 25 J in 250 and 900 psec pulsewidths. Experiments were performed at 1.06 microns and with doubled light at 5320 Å.** Wavefront distortion at the output was less than λ/4 and the linewidth was < 0.15 cm^{-1}. Some 2200 shots were made, 2/3 onto targets while the remaining 1/3 were used in system development and maintenance.

Installation of Faraday rotators this spring allowed adding amplifiers and raising the available energy to 100 J. This system is shown pictorially in Fig. 4 and schematically in Fig. 5. The 64 mm rod amplifier has been removed and replaced with a 44 mm aperture disc amplifier which has allowed us to deliver 100 J on target. Most of the 600 shots with disc amplifiers have been at 900 psec and as before, 2/3 have been on targets. Wavefront distortion for this configuration is < 1.5λ.

Operational experience has been that the 45 mm glass rod accumulates an objectional amount of self-focusing damage over 500-600 shots, setting an expendable materials cost of $10 - 12 per shot. No other predictable, systematic degradation has been found, although two Pockel's cell crystals and one glan prism have been damaged over the past year.

Operation of the isolation system has been trouble-free. Faraday rotator solenoid currents are routinely monitored and if found to be of tolerance, the outgoing laser pulse is killed by inhibiting the second Pockel's cell. In addition, the oscillator bank is crowbarred. In the few cases where either a rotator drive cable has failed or trigger power supplies have been unplugged, these measures have adequately protected the system.
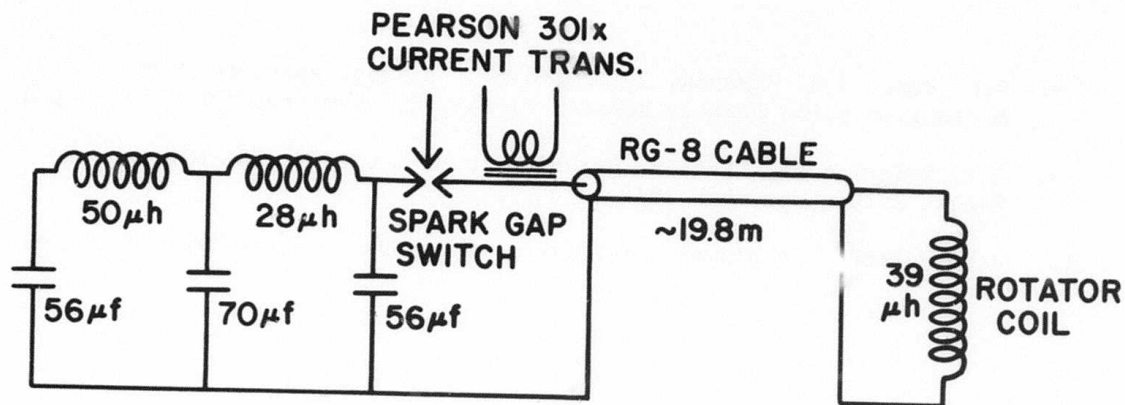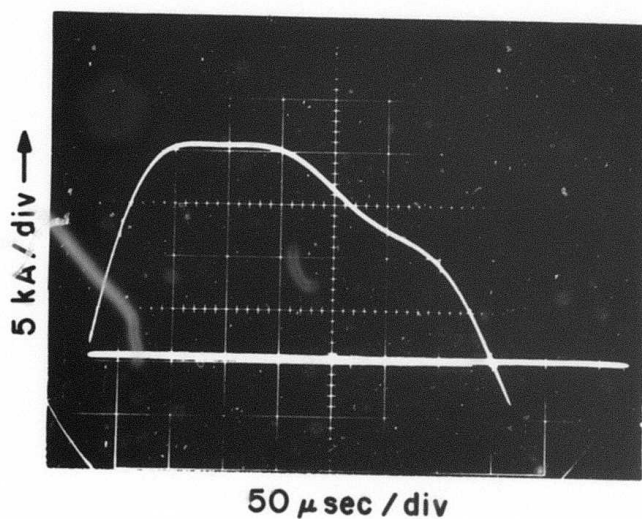
REFERENCES

1. P. Kelley, "Self Focusing of Optical Beams", Phys. Rev. Letters, Vol. 15 (Dec. 1965) p. 1005-1008.

2. M.A. Duguay and J W. Hansen, "Measurement of the Nonlinear Index n_2 of Glass using Picosecond Pulses", NBS Special Publication 341 (1971), 3rd ASTM-NBS Symposium on Damage in Laser Materials.

3. J.M. McMahon, "Damage Measurements with Subnanosecond Pulses", (1972) NBS Special Publication 372, 4th ASTM-NBS Annual Symposium on "Damage in Laser Materials", Boulder, Colorado, June 1972.

4. J. Marberger, 5th ASTM-NBS Symposium on "Damage in Laser Materials", Boulder, Colorado, May 1973.

5. J.F. Holzrichter, J.M. McMahon, C.M. Dozier, E.A. McLean, D.J. Nagel, J.A. Stamper, F.C. Young, "Laser-Target Interaction Experiments at NRL", Am. Phys. Soc., Monterey, California 13-16 Nov. 1972.

6. R. speck and E. Bliss, Conference on Laser Engineering and Applications, Washington, D.C., May 1973.

7. K. Büchl, K. Eidmann, H. Salzmann and R. Siegel, "Spectral Investigation of Light Reflected from a Laser Produced Deuterium Plasma", Appl. Phys. Lett., Vol. 20, 1, pg. 3-4, 1 January 1972.

8. J.P. Letellier "Parallel Plate Transmission Line Pockel's Cell", NRL Report 7463, October 12, 1972.

9. O.C. Barr, J.M. McMahon, J. Trenholme, "A Large Aperture High Extinction Ratio Faraday Rotator Isolator", submitted for publication.

10. J.F. Holzrichter, "Faraday F tation in EY-1 Glass", NRL Memorandum Report 2510, September 1973.

11. John McLeod, Los Alamos Scientific Laboratory, private communication.

PEARSON 301x
CURRENT TRANS.

RG-8 CABLE

50 μh 28 μh

SPARK GAP
SWITCH

~19.8 m

56 μf 70 μf 56 μf

39
μh

ROTATOR
COIL

(a)

5 kA./div →

50 μ sec / div

(b)

Fig. 1 - (a) Driving circuit for Faraday rotator module. The circuit
inductances are slightly 'tuned' from the indicated values to compen-
sate for component variations and give the most constant peak current.
(b) Rotator current obtained with this configuration at a nominal value
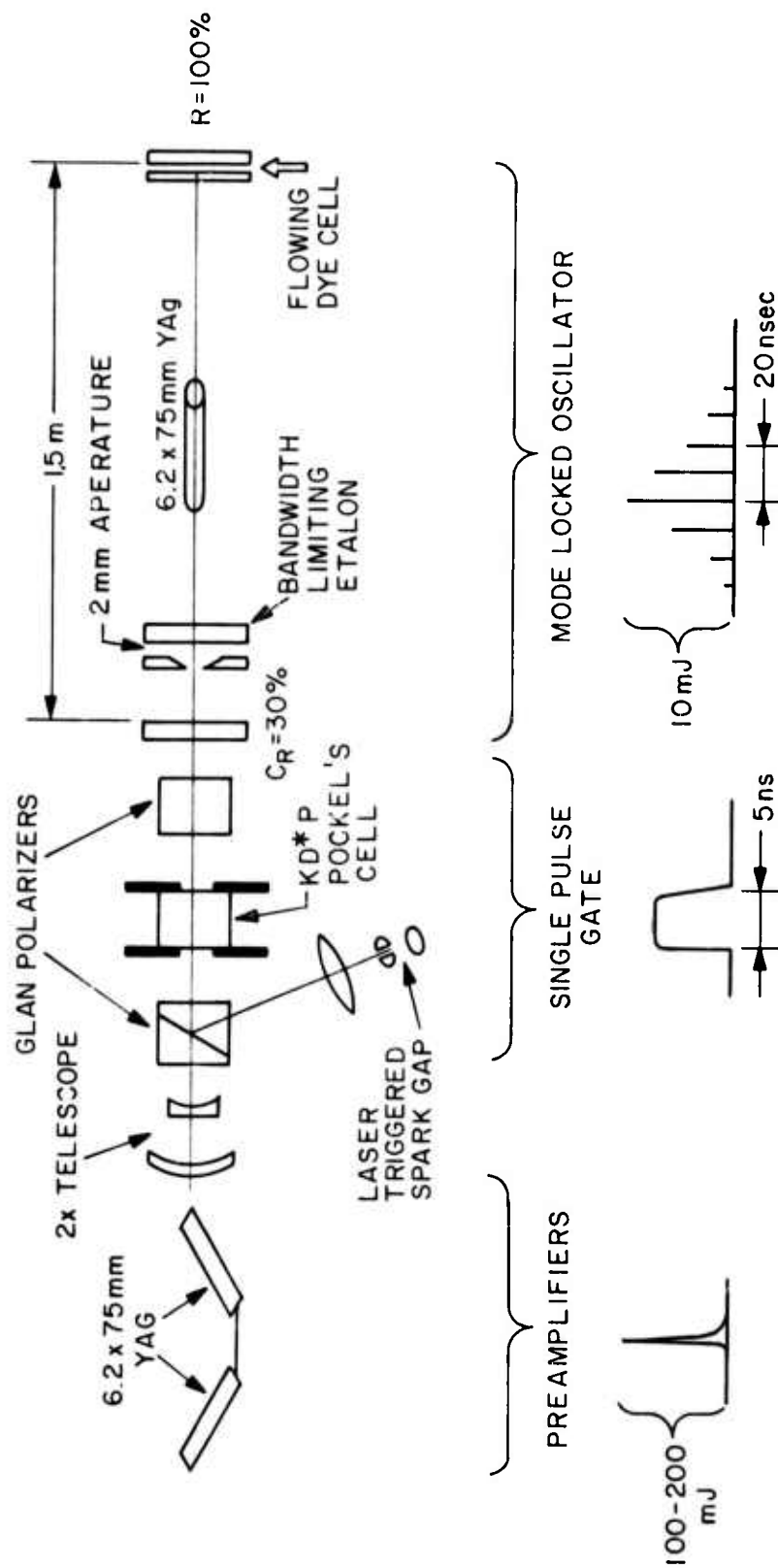of θ = 45°.

D-10

Fig. 2 - Schematic of the Nd:Yag short pulse generator. With no restriction of the bandwidth the oscillator would produce a train of 15 psec pulses. By narrowing the bandwidth with Fabry-Perot etalons, pulses as long as 900 psec have been obtained.
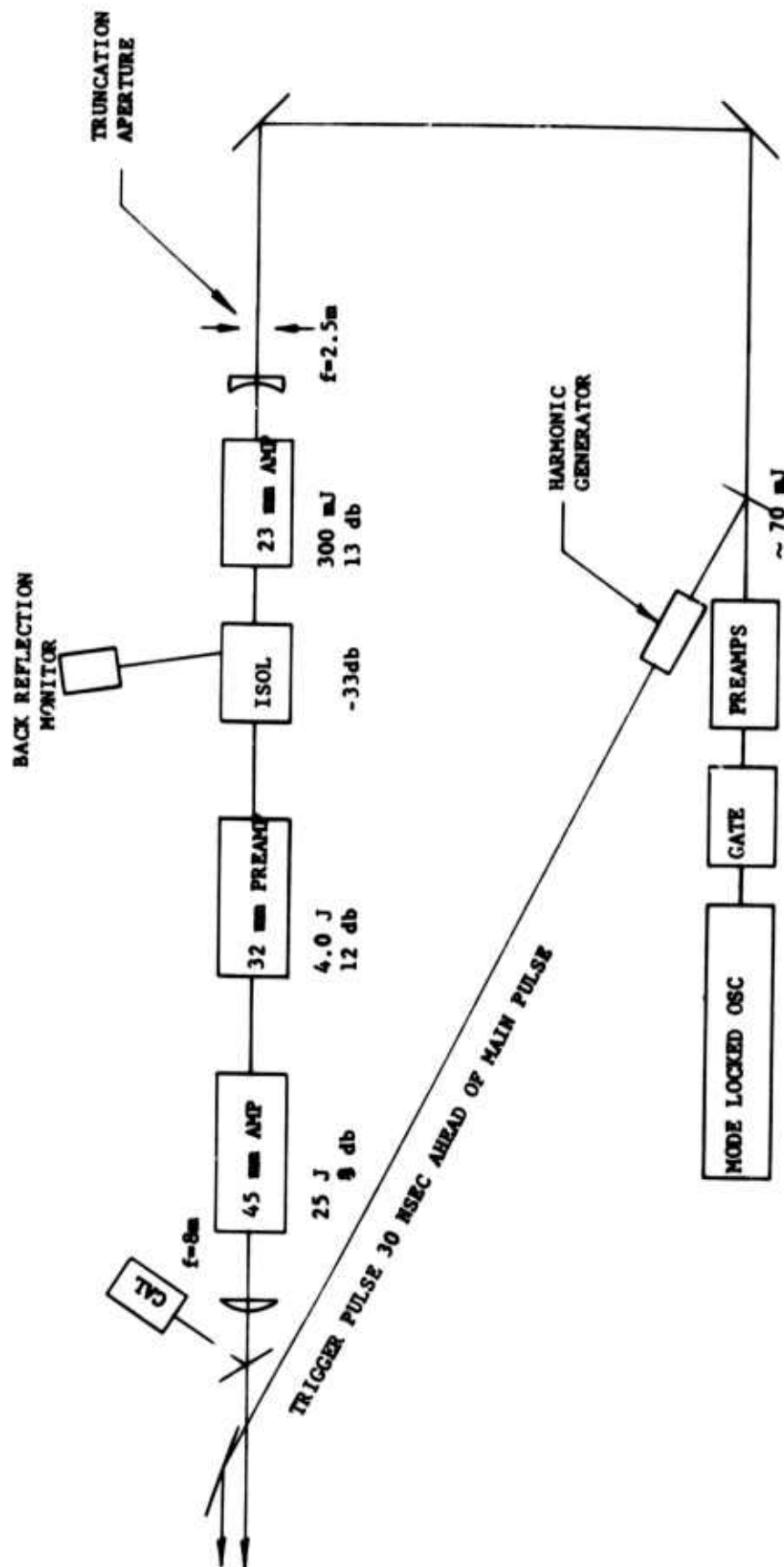
D-11

Fig. 3 - Schematic of the system through the rod amplifier stages with the two stage Pockel's cell isolation installed. As shown, the system has routinely produced 10^{11} watt pulses of near-diffraction limited beam quality.

D-12

Fig. 4 – View of the complete system with disc amplifiers and Faraday rotators as used to produce 100 – 200 J pulses.
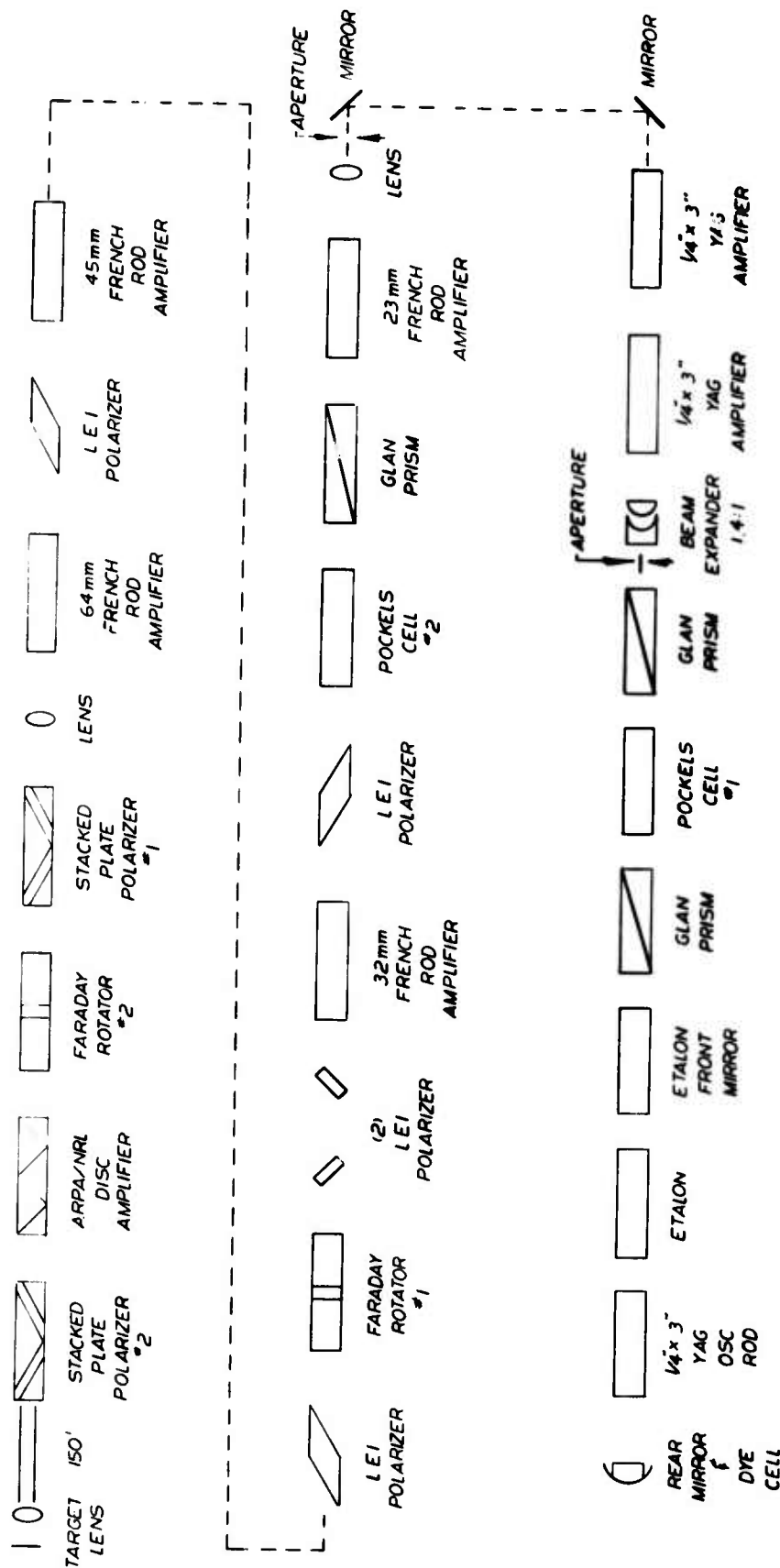
Fig. 5 - Block diagram of the configuration shown in Fig. 4. The 64 mm rod amplifier has been replaced by a 44 mm aperture disc amplifier which provides equivalent output with much greater reliability.

A Glass-Disk-Laser Amplifier

J. M. McMAHON, J. L. EMMETT, J. F. HOLZRICHTER, and J. B. TRENHOLME

A Glass-Disk-Laser Amplifier

J. M. McMAHON, J. L. EMMETT, J. F. HOLZRICHTER, AND J. B. TRENHOLME

Abstract—The details of the analysis, design, and operation of a Nd-glass-disk-laser amplifier which has been constructed at the Naval Research Laboratory are presented. Gain and fluorescence measurements have been compared to theoretical predictions; these show that 0.6-J/cm³ energy storage is achieved in the disk (assuming a cross section of 3.0×10^{-20} cm²). The effects of unsuppressed parasitic oscillations are demonstrated and an effective method of preventing their occurrence is shown. The disk amplifier has demonstrated 320-J output in a 1-ns pulse with 110-J input.

I. INTRODUCTION

HIGH-ENERGY short-pulse lasers are presently of great interest for experiments with plasmas, X rays, and controlled fusion. The designer who contemplates the construction of such a system is presented with major engineering problems, particularly with the final amplifier. This paper deals with the details of the analysis, design, and operation of a glass-disk-laser amplifier which serves as the output stage of a large laser system.

Historically, solid-state lasers have been constructed using rods as the active elements. When the designer turns to larger rods as he strives to increase laser output, he finds that rod fabrication rapidly becomes more difficult as the size increases. In addition, the thermal relaxation time of the rod becomes large, the pump uniformity is poor, and self-focusing of the laser beam in the long path through the rod causes destructive damage. These problems combine to make Nd^{3+}–glass-rod amplifiers undesirable above a diameter of about 4 cm.

The disk laser [1], in which the active material is in the form of separate slabs set at Brewster's angle to the beam, offers an attractive means of avoiding the problems that beset large-rod systems. This was first discussed by Swain *et al.* [2]. Disks may be made in sizes sufficient to amplify beams much larger than those practical with rods. Fabrication of the disks is relatively easy, and since the disks can be pumped through their faces, pumping uniformity is greatly improved. Damage to one disk due to self-focusing or other causes does not destroy the entire amplifier. Also rapid thermal transport through the disk faces reduces the thermal time constant compared to a rod of equivalent aperture size (for diameters much greater than the disk thickness).

Disk lasers are not without their own set of problems. The lower average density of active material in a disk-amplifier cavity may reduce the pump coupling efficiency, and the long-gain paths available in the individual disks may lead to parasitic-oscillation problems, although parasitic problems arise in any laser medium when the gain across a characteristic dimension is large. A disk laser will be more complicated (and thus more costly) than a rod laser. Finally, an important practical difficulty is the problem of keeping the many optical surfaces in a disk amplifier clean.

In the following sections gain and fluorescence measurements on the Naval Research Laboratory's (NRL) disk amplifier are presented. The results of these measurements are compared to theoretical predictions. We show that a relatively high pumping efficiency has been achieved. The effects of unsuppressed parasitic oscillations are demonstrated, and an effective method of preventing their occurrence is shown.

II. THE NRL DISK LASER

A disk-laser amplifier has been constructed and operated at NRL. This laser is designed to act as the final amplifier following a modified CGE VD-640 Nd^{3+}–glass-rod laser system.[1] The output of the rod system is a 100-J pulse of less than 1-ns duration in a 6-cm-diameter beam. The beam profile is not an exact Gaussian, but it has a smooth variation of power with radius, and only small amplitude ripples due to diffraction (this lack of abrupt spatial changes in amplitude is necessary to avoid self-focusing damage in the system). The disk amplifier was designed to have an output of 400 J with this input pulse.

Since the terminal level of the laser transition in laser glass does not have time to empty during a subnanosecond pulse, a maximum of half of the stored energy can be extracted in a single-pass amplifier. The input-energy density to the disk amplifier is close to one saturation flux, thus less than this maximum will be extracted. To raise the 100-J input to 400 J means that 300 J must be extracted or that about 1000 J must be stored in the disk amplifier. Measurements by Swain *et al.* [2] and preliminary coupl-

[1] The disk amplifier was designed to be driven by a modified Companie General d'Electricité Model VD-640 laser system. A specially constructed Nd:YAG mode-locked oscillator, pulse switch-out system, and two Nd:YAG preamplifiers provide an 80-mJ pulse, 20 ps–1 ns in duration. This pulse is spatially shaped to minimize Fresnel fringing in the glass amplifier system. The glass system amplifies this pulse to the 100-J level (for 1-ns pulses) and provides a diffraction-limited pulse with self-phase modulation kept less than a 1.0 cm⁻¹.

Fig. 1. Individual disk-lamp holder (scale is in inches). The disk-amplifier assembly consists of eleven of these holders placed end to end in a zigzag pattern. Twenty-two lamps each 60-in long are slid through the disk holders to completely surround the disks. Separate top and bottom reflectors are placed around the disk holders. All of the metal surfaces are gold-plated.

Fig. 2. Small-signal-gain measurement setup. A Chromatix 1000-C Nd:YAIG laser was used to probe the disk-amplifier gain. The wavelength of the probe could be adjusted from 0.96 μ to 1.079 μ.

ing efficiency estimates that 0.6 J/cm^{+3} could be stored in the glass indicated that $\sim$ 1700 cm^{+3} of glass would be required. These considerations led to a design consisting of 11 disks of Owens-Illinois ED-2 glass set at Brewster's angle. Each disk is a 14- $\times$ 7-cm ellipse of 2-cm thickness. The beam path length through the disks is thus 26 cm.

The pump source for the disks consists of 22 linear flashlamps with their axes parallel to the beam axis. The flashlamps are placed around the disks in a close coupled arrangement (Fig. 1). The lamps have a 145-cm arc length, and are 10-mm ID by 14-mm OD xenon lamps of conventional design filled to 450 T. Each lamp is driven by a separate 42-μF 20-kV capacitor module through a 300-μH inductor. These circuit values are chosen [3] to give a critically damped pulse whose width (340 μs) is optimal for pumping ED-2 glass, and to insure a lamp life of more than 10^4 shots in free air (the lifetime is reduced in the laser cavity due to self-loading). The total stored energy in all the modules is 185 000 J at 20 kV.

The cavity structure consists of 11 disk-lamp holders and a two-piece outer reflector (Fig. 1). The metal surfaces were gold-plated to provide high pump-band reflectivity, low UV reflectivity, and chemical inertness in a high-light-flux environment. The cavity is purged with gaseous nitrogen to cool the disks between shots and to remove oxygen from the cavity in order to prevent shock-wave formation [4].

The operation of large laser systems is limited by optical damage caused by the intense optical beam. For pulsewidths of several nanoseconds or less, self-focusing damage is more serious than surface or bulk damage. The flux levels at which our system operates do not exceed the surface and bulk-damage thresholds of the glass used. We
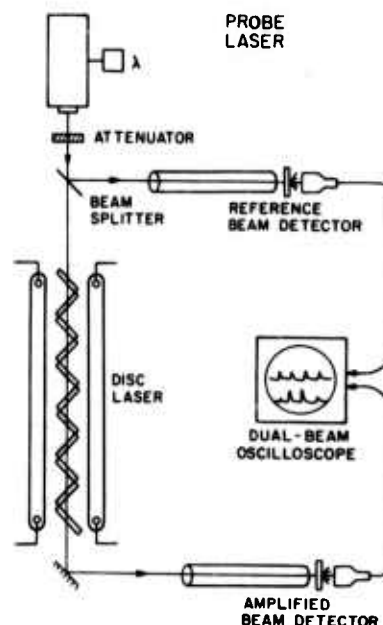
have observed that self-focusing damage is due to wavefront distortion arising from dirt or optical imperfections rather than collapse of the beam as a whole.

III. ENERGY-STORAGE MEASUREMENTS

When the disk laser was first operated, the gain achieved at high pump levels was considerably less than expected. This difficulty was traced to the presence of parasitic oscillations (free lasing) within the individual disks. These parasitics were eliminated by coating the disk edges with an absorbing glass coating. The disk amplifier was then able to meet the design of goal of 0.6-J·cm^{-3} energy storage.

The disk-laser problem was diagnosed by measuring the small-signal gain of the amplifier. For small signals, the amplifier output intensity is given by

$$I = I_0 \exp(\sigma nl - \gamma l)$$

where I_0 is the input intensity, σ is the stimulated-emission cross section of the laser material at the signal wavelength (3 $\times$ 10^{-20} cm^2 for ED-2 at 1.064 μ), n is the inversion density, l is the length through the amplifying material (26 cm in this case), and γ is the absorption coefficient. By measuring the pumped and unpumped gain (loss), n may be determined if σl is the same in both cases. The stored-energy density is then found from n.

The gain measurements were made using a Chromatix 1000-C Nd^{3+}:YAIG laser operating in a TEM$_{00}$ spatial mode as a probe source (Fig. 2). This laser was tuned to the desired transition, and the beam was passed through the disk amplifier. The beam was about 5 mm in diameter and passed along a line about 2 cm from the center of the

disks. A portion of the beam was split off before passage through the amplifier for use as a reference. The reference beam and the amplified beam was measured by S1 biplanar photodiodes[2] with diffusers and pump light shields. Saturation at the detectors was carefully avoided. The probe laser was operated in the pulsed, multiply Q-switched mode. It emitted six to ten pulses at 20-μs intervals. The time variation of the disk amplifier gain could thus be followed.

Measurements were first performed to determine if the low gain observed in the disk amplifier was due to a pump-induced loss (that is, to an increase of γ during the pump pulse). Such a loss might be due to formation of transient color centers in the glass [5], to an induced absorption in the air path, to pumped birefringence in the disks, or to other unknown causes. However, measurements at 0.946 and 1.12 μm showed neither gain nor loss, and measurements at 1.052, 1.064, 1.074, and 1.079 μ showed small gains which were proportional to the values of σ at those wavelengths which could be inferred from published fluorescence data of this glass [6]. Thus any pump-induced loss was required to have exactly the same line shape as the gain. This appeared unlikely, and so an induced loss was rejected as the cause of the trouble.

Consequently, the difficulty had to be a result of low inversion, which could be due either to fluorescence amplification or to parasitic oscillations. Calculations (outlined later) show that fluorescence amplification causes only a small decrease in inversion for the disk size and gain used in the NRL laser. Thus parasitic oscillations in the disks were the suspected cause.

Parasitic oscillations in disks are expected to be sensitive to the absorption at the disk edge. A series of tests were therefore run with different edge treatments on the disks. For each treatment, a series of measurements was made at different input energies to the disk amplifier. At each energy, the gain was found as a function of time during the disk pump pulse. Fig. 3 shows a typical set of these experimental curves, plotted as per-disk gain versus time.

The effect of different edge treatments is shown in Fig. 4. This shows the maximum stored-energy density achieved as a function of bank energy. A fine-ground acid-etched surface next to a gold-plated surface begins oscillating at an extremely low stored energy of 0.15 J/cm³. Since no more energy may be stored once oscillation starts, the stored energy is limited to a very low value. Replacing the gold surface with blackened copper raises the threshold to 0.43 J/cm³, but oscillation still occurs. When the edge of the disk is coated with a black glass,[3] no oscillation is observed and the desired energy density is achieved. The observed dependence of maximum stored
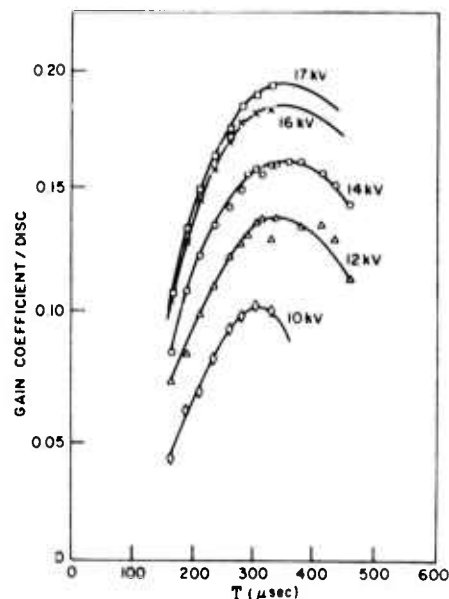
Fig. 3. Disk-gain coefficient as a function of time and bank voltage. Total stored energy in disk-amplifier capacitor bank is 185 kJ at 20 kV.
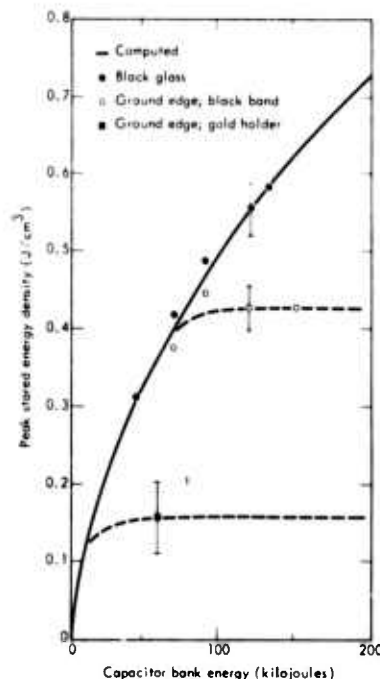

Fig. 4. Comparison of experimental and calculated energy density in the disk laser. The solid line shown is the calculated energy density in the disks versus flashlamp input energy. The solid round points show the measured energy storage (gain) as a function of bank energy for black-edged disks. The open round and solid square points are experimental measurements of gain saturation due to parasitic oscillation in uncoated disks.

energy on edge treatment shows conclusively that the low gain of the disk laser was caused by parasitic oscillation.

Additional measurements were performed to verify the presence of parasitic oscillations in the disk. The 1.06-μm radiation out of the major and minor axes of one of the
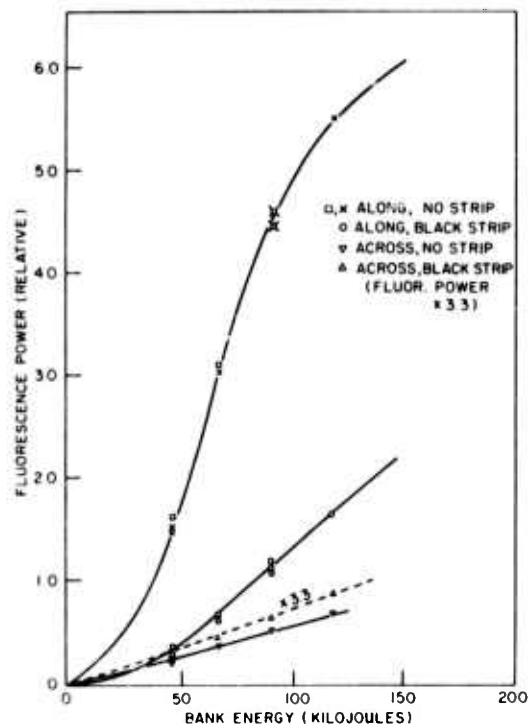
Fig. 5. Peak fluorescence power through disk edge as a function of edge preparation. Coatings were not applied to the disk edges for the data presented here. Along and across refer to observation direction along the disk major axis or across it (i.e., along the disk minor axis). Notice that the across data taken with the black strip between the disk edge and the holder are magnified by 1.386×.

elliptical disks was monitored by means of a fiber-optic light guide leading to a monochromator and an S1 photomultiplier. Small flats were polished on the edges of the disk, and the fiber bundle was optically contacted to one or the other with a high-viscosity silicone fluid. The disk was pumped in its normal position inside the disk amplifier. Neutral density and bandpass filters were required in addition to the monochromator in order to maintain linearity and reject flashlamp radiation. Electric and magnetic shielding of the electronics were also employed.

The peak 1.06-μm output from the major and minor axes is plotted in Fig. 5 as a function of bank energy. The large, rapidly rising signal along the major axis when a fine-ground acid-etched edge is next to a gold-plated surface is evidence for an oscillation in the disk. The smaller, linear output with a black-copper surface is interpreted as a normal fluorescence signal.

IV. THEORETICAL ANALYSIS AND COMPARISON WITH EXPERIMENT

The techniques that have been used in the design and analysis of the disk amplifier include an optical power-flow analysis of the pumping in the laser head, a calculation of the effect of fluorescence amplification on the achievable inversion, and a determination of the inversion limits set by parasitic oscillations in the disk amplifier.

Details of these calculations and comparisons with experiment follow.

The pumping in the disk laser was analyzed using a model of the spectral emission and absorption of the xenon flashlamps [7] and a versatile optical power-flow analysis program [8]. The physical details of the lamps, disks, and disk-lamp support structures were modeled in detail, using the capability of the power-flow program to accept complicated, varied geometries. The optical rays which are followed through the laser structure were started uniformly at random throughout the lamp volumes. Each ray carried spectral power data corresponding to two-hundred wavelength intervals from 2000 Å to 1.2 μ. The initial power in each interval was set to correspond to the xenon plasma emission at the interval's center wavelength. The ray was then followed through the laser geometry. The ability to treat each wavelength interval separately allowed the wavelength-dependent reflectivity of the gold cavity surfaces and the complicated glass absorption spectrum to be treated accurately. The amount of power absorbed by the laser glass, the cavity surfaces, and the lamp plasma were thus found. Since the flashlamps absorb part of their own radiation, both before and after its passage into the cavity, it was necessary to make separate calculations to determine the initial absorption of the rays before they leave the lamps and the subsequent absorption of the rays as they pass through the lamps, glass, etc. The initial internal absorption was found by doing a separate calculation with a completely absorbing medium surrounding the lamps. A self-consistent calculation was then used to find the conversion efficiency from electrical power in the lamps to pumping in the glass. The principle of the self-consistent calculation is described in the appendix. The calculated values of peak inversion as a function of bank energy were fitted to the experimental results by varying the one free variable in the calculation. This variable (called Q) represents the combined uncertainties in the absorption quantum efficiency, stimulated emission cross section, fluorescent decay in the glass, and inaccuracy in the flashlamp model. Nominal values are assumed for the components of Q, and deviation from these values is reflected in a variation of Q from unity. A factor of 1.06 was also included because the experimentally probed central region of the disks had a higher energy density than the disk average (this factor was found by a power-flow calculation in which the disk was divided into a number of small segments). The match for a Q of 0.5 is shown by the solid line in Fig. 4. Agreement is good, but the nonunity value of Q indicates that a problem exists. The absorption quantum efficiency (not to be confused with the fluorescence conversion efficiency) needed to give $Q = 0.5$ is inconsistent with measured values [9] of unity. A more likely source of the discrepancy is the flashlamp model, which is based on sparse experimental data. The fluorescent decay was modeled by a single 300-μs decay, which may be wrong. It is also possible that the assumed value of the stimulated-emission cross section σ used to
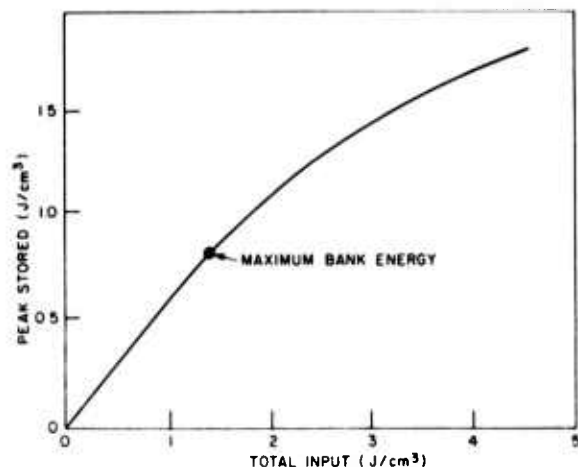
Fig. 6. Effect of fluorescence amplification on peak stored energy versus total absorbed energy, calculated for a disk similar to that in the NRL amplifier. The reduction is only 3 percent at the maximum pump energy.
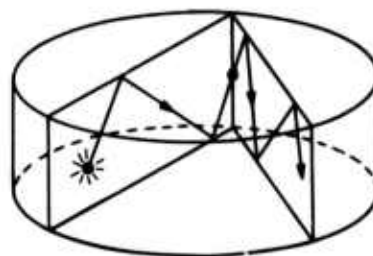

Fig. 7. Ray path which bounces off both laser-disk face and edge. Between edge reflections, the path zigzags in a plane perpendicular to the faces. The path changes to a new plane at each edge reflection.

relate small-signal gain to stored-energy density is incorrect (3.0×10^{-20} cm² was used).

The fluorescent loss rate in a laser disk is increased above the normal rate when the gain across a disk is large enough that spontaneously emitted radiation is significantly amplified before it exits from the disk or is absorbed at the edge. This process has been studied in detail [10] using the same optical power-flow program used in the pumping analysis. A negative loss coefficient was used in an elliptical disk to simulate the optical gain of the pumped laser material. A Lorentzian-line profile was assumed for the gain, since this gives a reasonable approximation to the more complicated actual line shape. This calculation yielded the nonlinear relation between energy density and loss rate in the disk. The differential equation for the inversion was then integrated, assuming a half-sine pump pulse and the calculated loss rate. The peak inversion resulting from this integration is plotted against the pump energy in Fig. 6 for a pump pulsewidth equal to the fluorescent lifetime. The point on the curve corresponds to the operation of our laser at peak bank energy. The reduction in peak inversion is only about 0.03 of the peak value in the absence of fluorescence amplification, and thus can be ignored. However, fluorescence amplification arises rapidly as the across-disk gain increases, and therefore may become significant for larger disk lasers.

Lasers are subject to parasitic oscillations if careful measures to suppress the oscillations are not taken. These were first noticed by Swain et al. [2]. Such oscillations arise because of the large gain available in a laser structure. They are harmful because once a parasitic oscillation has begun, no more inversion increase is possible in the oscillating-mode volume. This problem has also been analyzed [10]. A simple analysis was used which ignored the effects of phase and diffraction, since these effects will be small in a resonator such as a laser disk which is much larger than a wavelength. The gain along a path such as

the one shown in Fig. 7 was calculated as a function of the face and edge intersection angles, assuming uniform gain in the disk. The lowest loss path is the one which lies in a plane across the diameter of the disk, and which hits the faces at the smallest angle from the face normal which still allows total internal reflection. The only losses on such a path come at the edge reflections. At the oscillation threshold this edge loss must just cancel the path gain. Since the path length for this path is the disk refractive index n times the diameter D (assuming the disk is in air), we must have

$$R \exp{(nD\alpha)} = 1$$

at the oscillation threshold, where α is the gain coefficient in the laser material and R is the edge reflectivity (at the complement of the face angle for total internal reflection). For example, if αD is equal to 3 (i.e., the across-disk gain is 20), and the index is 1.56, then the reflectivity must be less than 1 percent to avoid oscillation. The most practical method of achieving the required low reflectivities is to coat the edge with an absorbing substance with an index slightly above that of the laser material (an index lower than the laser's allows lossless oscillations near the disk periphery). The reflection will then be due only to the refractive-index difference at the disk–coating interface, and thus can be kept small. From a practical standpoint, the coating should match the disk's thermal-expansion coefficient (for ease of application), and it should be able to withstand large power loadings. Even if the coating absorbs no pumping radiation, it must absorb about ⅓ of the energy stored in the disk. This loading is due to fluorescent loss, which mostly goes to the disk edge.

The effects of unsuppressed parasitic oscillation are illustrated in Fig. 4. The theory that is given in [10] indicates that at a certain gain threshold oscillation begins and the disk gain remains constant. However, the fluorescence that is observed through the disk edges (see Fig. 5) does not show a knee, or threshold point, which would indicate that oscillation had begun. This indicates that the parasitic-mode structure in the actual laser disks is somewhat different than that analyzed in the simple model. In addition, the calculated edge reflectivity that is necessary to cause oscillation at $\alpha l = 0.95$ ($\rho_E = 0.43$ J/cm³) is about 30–40 percent. This is higher than preliminary measurements on the internal smooth ground

edge would indicate (~10 percent). The parasitic model assumed spatially uniform gain in the disks, which is not the case. An oscillating mode may develop in the heavily pumped face regions of the disk. This mode should not seriously deplete the overall inversion, but it may contribute to the observed large parasitic-fluorescence signal. Additional study on the parasitic-mode structure and the internal surface reflectivities of laser media is required.

Parasitic oscillation will set a definite upper limit to the size of disk lasers, since oscillation suppression becomes rapidly more difficult as the across-disk gain rises. With present suppression methods, an across-disk gain at the fluorescent-line peak of exp (3) probably represents an upper limit. The construction of larger lasers awaits the development of extremely good parasitic suppression methods, or requires some sort of segmenting of the disk to avoid long across-disk paths.

V. DISK-AMPLIFIER PERFORMANCE

The disk amplifier was assembled with black edge-coated disks and its performance was tested by using the NRL modified CGE VD-640 laser system as an input source. The output energy as a function of input energy was compared to a theoretical model which is based on a rate-equation approach similar to that first formulated by Avizonis and Grotbeck [11]. This can be used to predict the output of our amplifier if several assumptions are made.

1) The amplifier is a three-level amplifier, because the lower-level decay time is much longer than the pulse duration. The measurements which have been reported all give values for this decay time in excess of 5 ns [12]–[15].

2) The pulse duration is long compared to T_2^*, the upper-level cross-relaxation time. From the theoretical treatment of Basov *et al.* [16] and Gobeli *et al.* [17] on amplifying ultrashort pulses, one can estimate that T_2 must be shorter than $\simeq 30$ ps, or operation at their reported level would not have been possible.

In this case an equation for the rate of energy addition to the pulse can be derived in the form

$$\frac{dE(Z)}{dZ} = \frac{N}{2}\left\{1 - \exp\left(\frac{-2E(Z)}{E_s}\right)\right\} - \gamma E(Z) \qquad (1)$$

where $E(Z)$ is the energy density at a given distance Z; N is the upper-level energy density (in joules/cubic centimeter); E_s is the saturation flux, which is equal to $h\nu/\sigma$, and is ~7 J/cm² for the Owens-Illinois ED-2 glass used in the amplifier; and γ is the loss coefficient. As has been recently pointed out by Fill and Finckenstein [18], this equation can be put in the convenient dimensionless form

$$\frac{dE(Z)}{d(\alpha Z)} = \tfrac{1}{2}(1 - \exp(-2E(Z))) - \frac{\gamma}{\beta} E(Z)$$

where $E(Z) = E(Z)/E_s$ and $\beta = \alpha N/h\nu$.

For input energies of up to 75 J, using values of gain (derived from the small-signal experiments) equal to 7.3 ×
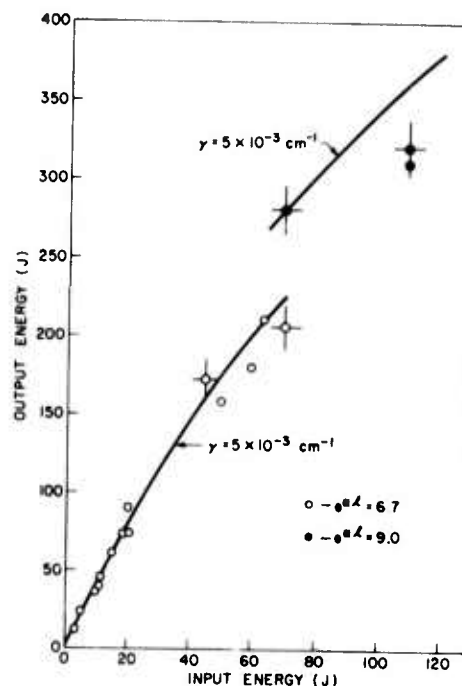

Fig. 8.   Disk output energy as a function of input energy. Both 0.25- and 1.0-ns pulses are used as input pulses. Gain values of $\alpha l = 1.9$ and $\alpha l = 2.2$ were used. The loss coefficients γ are explained in the text. At the higher gain level of $\alpha l = 2.2$ with 75-J input energy, the disk performs as expected. At 110-J input, the apparent disk gain falls due to the increased divergence of the input beam.

10^{-2} cm⁻¹ and 8.4×10^{-2} cm⁻¹ and a loss value of $(5 \pm 2) \times 10^{-3}$ cm⁻¹, (for both 250-ps and 1-ns pulses), this equation describes the disk amplifier very well (Fig. 8). The loss coefficient of 5×10^{-3} cm⁻¹ (a transmission of 88-percent overall) was measured both with a low-power Nd:YAG laser and with the output from the 64-mm rod-amplifier stage. This loss is due mainly to surface scattering, birefringence in the preceding driver stages, and angular misalignment in the disks themselves.

At 100-J input the disk-amplifier output was less than expected. The properties of the 64-mm rod source were investigated to account for the reduced disk output, and it was found that a mechanism exists which degrades the coherence and collimation of the beam in the final rod amplifier. Fig. 9 shows time-averaged shear plate [19] interferograms of the wavefront for intensities below and above the onset of the effect. The ideal wavefront at the output from the 64-mm rod amplifier is a spherically divergent wave and the lower intensity case [Fig. 9(a)] shows a reasonable approximation to this. The higher intensity case (20–30-GW/cm² peak power density) shows gross wavefront distortion [Fig. 9(b)]. Burn patterns at this level showed a divergence so large that it was geometrically impossible for the beam to pass through the disk amplifier. The nature of this beam degradation is not understood. It was observed, however, that the output beam from the disk amplifier was well-behaved at power densities well above those at which the beam from the rod system had become unusable [20].
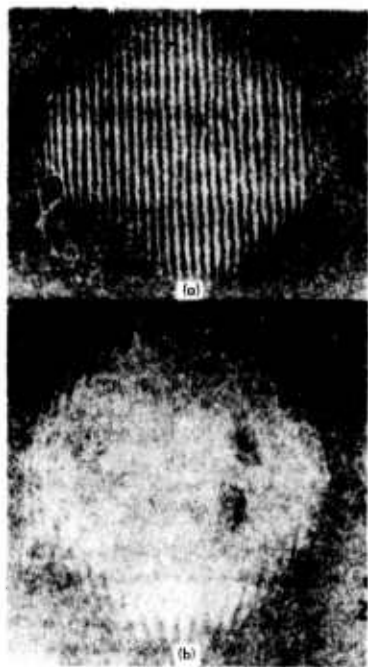
Fig. 9. Shearing-plate interferograms of the output from the 64-mm rod amplifier. (a) Interferogram shows a nearly spherically diverging beam from the amplifier. This can be corrected with an 8-M focal-length lens to yield ≤1 wavelength of distortion across the beam. (b) Interferogram shows gross wavefront distortion present when the self-focusing threshold is reached. The figures were photographed from burn patterns on exposed and developed copy paper, supplied by Hadron, Inc., 800 Shames Drive, Westbury, N.Y.

Energies were measured using large carbon-cone calorimeters[4] preceeded by glass attenuators which reduced the input to the calorimeter to a level at which breakdown in the calorimeter did not occur (<50 mJ/cm²). The attenuation factor of the filters was checked in a separate experiment. The attenuation was found to remain constant up to ≃25 J/cm² where surface breakdown occurred. The estimated accuracy of the energy measurements is ~5 percent.

VI. Summary

The present system has shown that a large disk amplifier can be pumped to an energy density that is comparable to or greater than equivalent diameter rods (the 64-mm rod in the system is pumped to ~0.3–0.5 J/cm³). In addition, the optical quality is excellent, the thermal properties with N_2-gas cooling are equivalent to those of a 64-mm rod which is liquid cooled, and the calculated pumping uniformity shows a gain profile which is smooth to ± 10 percent. Methods of analyzing and solving the parasitic-oscillation problem within single disks have been given. Additional work on self-focusing in these systems must be done, although small-scale self-focusing damage should be no worse a problem than in an equivalent length of solid glass.
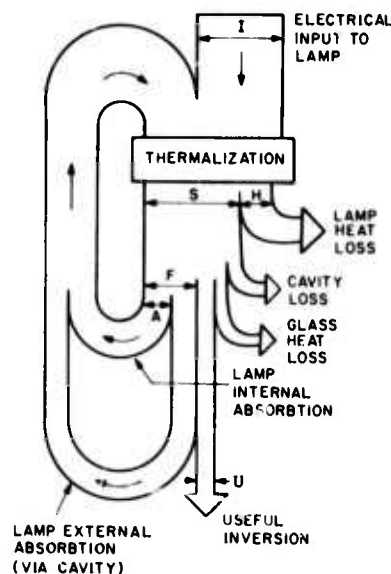
Fig. 10. Diagram illustrating the flow of power in a laser cavity. The return of power to the lamps after passage through the cavity (lamp external absorption) requires a self-consistent calculation of the electrical-to-inversion transfer. See text for description.

Appendix
Self-Consistent Pumping Calculation

The principle of the self-consistent calculation is illustrated in Fig. 10. The computer code [8] operates by tracing the power flow from the lamp terminals to optical radiation.

The electrical input power I and the radiation that is absorbed (both before escape from the lamp and after passage through the cavity and back into a lamp) combine to produce the total power input to the lamp. These sources are assumed to be equivalent. This means we have assumed rapid thermalization of the reabsorbed optical energy and spatial equivalence of the electrical input and the reabsorbed radiation. The total power input is converted into radiation S inside the flashlamp, and heat loss H to the lamp wall. An amount of radiation A is absorbed inside the flashlamp; the remainder $(S-A)$ exits from the lamp. Some of the exitting radiation is lost by absorption in the cavity, some is absorbed by the glass, and some is absorbed by the flashlamps. The power absorbed by the laser glass does not all become useful inversion; a portion is lost as heat in the glass instead of contributing to excitation of the ions (absorption quantum efficiency), and even when an ion is excited a fraction of the pump-photon energy is lost due to the energy difference between a pump photon and an emitted laser photon (quantum defect). The ray-tracing optical power-flow program automatically calculates the effects of the quantum defect, but quantum efficiency must be added later.

The efficiency we desire is the ratio of the inversion to the electrical input, or $\eta = U/I$. The power-flow program yields the radiation starting in the lamps S, the total initial internal lamp absorption plus the subsequent lamp reabsorption F, the useful inversion U, and (in a separate black-exterior run) the initial lamp internal absorption A.

We must find the electrical input I in order to calculate η. We have $I = S + H - F$, where H is the heat lost to the flashlamp wall. This loss must be found from the radiative efficiency of the flashlamps, which may be determined from the model of xenon flashlamps [7]. The radiative efficiency is $R = (S-A)/(S + H - A)$, so

$$H = (S-A)\left(\frac{1}{R} - 1\right).$$

Therefore,

$$\eta = \frac{UQ}{\dfrac{S-A}{R} + A - F}$$

where Q is the quantum efficiency (assumed constant with wavelength).

The self-consistent calculation of transfer efficiency is done for a number of input current densities. However, the flashlamp model derives the plasma state from the input current density alone, and does not allow for an increased energy input due to radiation reabsorbed from the cavity. It is therefore necessary to reduce the input current density so that the sum of electrical and radiation inputs is equal to the originally assumed electrical input. The electrical input must be reduced from $S + H - A$ to $S + H - F$, or from $(S-A)/(R + A - F)$ to $(S-A)/R$. Since the power goes as the 3/2 power of the current density [3], the current density must be reduced from the assumed value by a factor K which is given by

$$K = \left[1 - R\left(\frac{F-A}{S-A}\right)\right]^{2/3} \tag{2}$$

It should be added here that the lifetime of the flashlamps must be calculated from their total input power, which is equal to the total power density. The self-consistent relationship between transfer efficiency and instantaneous current density is determined by using the procedure described above.

The actual peak inversion in the laser material is determined as follows. An assumed power density in the lamps is multiplied by the transfer efficiency (which can be a function of power density) to find the pumping rate in the glass as a function of time. In practice, the transfer efficiency is assumed to be constant, corresponding to a power density equal to 0.72 times the peak power density. Calculations have shown this to be a good approximation. This pumping rate is used as the forcing function in the differential equation which describes the decay of the inversion (in general, this differential equation should include the effects of fluorescence amplification and parasitic oscillation [10]). The calculation is further simplified by assuming that the spontaneous fluorescence loss reduced the stored inversion to 0.66 of the value it would achieve with zero loss. This value of 0.66 is appropriate for a half-sine pump pulse of base width equal to the fluorescent lifetime of the material ($300 \mu s$), which is close to the situation in our laser. For this pulsewidth, a given inversion in

the glass is associated with a time integrated power density dissipated in the lamp. The current density which corresponds to this power density must be reduced by the factor K [1] to account for the reabsorbed optical power in the lamps. By using the results for a single flashlamp discharge circuit [3], one can work backwards from the corrected current density to find the stored capacitor bank energy. An additional 0.08 loss is included to account for the measured capacitor-to-bank transfer loss.

REFERENCES

[1] J. C. Almasi, J. P. Chernoch, W. S. Martin, and K. Tomiyasu, "Face pumped laser," G.E. Rep. to the Office of Naval Research, May 1966.
[2] J. E. Swain et al., "Large-aperture glass disk system," J. Appl. Phys., vol. 40, pp. 3973–3977, Sept. 1969.
[3] J. P. Markiewicz and J. L. Emmett, "Design of flashlamp driving circuits." IEEE J. Quantum Electron., vol. QE-2, pp. 707–711, Nov. 1966.
[4] R. C. Elton, "A study of radiation induced shock waves external to quartz discharge tubes and associated fracture problems," Plasma Phys. (J. Nuclear Energy, pt. C), vol. 6, pp. 401–404, 1964.
[5] E. Snitzer and R. Woodcock, "Saturable absorption of color centers in Nd³⁺ and Nd³⁺ laser glass," IEEE J. Quantum Electron., vol. QE-2, pp. 627–632, Sept. 1966; also R. J. Landry and E. Snitzer, "Ultraviolet-induced transient and stable color centers in self-Q-switching laser glass," J. Appl. Phys., vol. 42, pp. 3827–3837, Sept. 1971.
[6] D. K. Dustin, "Factors influencing the gain in neodymium doped laser glass," M.S. thesis, Dep. Elec. Eng., Rensselaer Polytechnic Inst., Troy, N. Y., 1969, p. 39
[7] J. B. Trenholme and J. L. Emmett, "Xenon flashlamp model for performance prediction," in Proc. 9th Int. Conf. High Speed Photography, 1970, p. 299.
[8] J. H. Alexander, M. Troost, and J. E. Welch, The Zap Laser Analysis Program, Systems, Science and Software Inc., 1971 (available from the Defense Documentation Center as AD-884-920), modified by one of the authors (J.B. Trenholme).
[9] L. G. DeShazer and L. G. Komai, "Fluorescence conversion efficiency of neodymium glass," J. Opt. Soc. Amer., vol. 55, pp. 940–944, Aug. 1965.
[10] J. B. Trenholme, "Flourescence amplification and parasitic oscillation limitations in disc lasers," Naval Research Lab. Mem. Rep. 2480, July 1972.
[11] P. V. Avizonis and R. L. Grotbeck, "Experimental and theoretical ruby laser amplifier dynamics," J. Appl. Phys., vol. 37, pp. 687–693, Feb. 1966.
[12] J. M. McMahon and T. H. DeRieux, "Laser glass testing at NRL," in 2nd ASTM-NBS Symp. Damage in Laser Materials, NBS Special Tech. Publ. 341, pp. 19–27, Dec. 1970.
[13] P. C. Magnante, "Influence of the lifetime and degeneracy of the ⁴I₁₁/₂ level on Nd-glass amplifiers," IEEE J. Quantum Electron., vol. QE-8, pp. 440–448, May 1972.
[14] W. E. Hagen, "Diffraction limited high radiance Nd-glass laser system," J. Appl. Phys., vol. 40, pp. 511–516, Feb. 1969.
[15] R. Dumanchin, J. C. Farcy, M. Michon, and P. Vincent, "Analysis of giant pulse amplification in Nd³⁺ doped glass," IEEE J. Quantum Electron., vol. QE-7, pp. 53–59, Feb. 1971.
[16] N. G. Basov, R. V. Ambartsumyan, V. S. Zuev, P. G. Kryukov, and V. S. Letokhov, "Nonlinear amplification of light pulses," JETP, vol. 23, pp. 16–23, July 1966.
[17] G. W. Gobeli, J. C. Bushnell, P. S. Peercy, and E. D. Jones, "Observation of neutrons produced by laser irradiation of lithium deuteride," Phys. Rev., vol. 188, no. 1, pp. 300–302, Dec. 1969.
[18] E. E. Fill and K. G. V. Finckenstein, "A comparison of the performance of different laser amplifier media," IEEE J. Quantum Electron. (Corresp.), vol. QE-8, pp. 24–26, Jan. 1972.
[19] See, for instance, M. V. R. K. Murty, "The use of a single plane parallel plate as a lateral shearing interferometer with a visible gas laser source," Appl. Opt., vol. 3, pp. 531–534, Apr. 1964.
[20] Operation of a tilted-slab laser at 50 GW/cm² has recently been reported: M. J. Lubin, J. M. Soures, and L. M. Goldman, "Large-aperature Nd-glass laser amplifier for high-peak-power application," J. Appl. Phys., vol. 44, Jan. 1973.